Inorganic Chemistry

Article

pubs.acs.org/IC

Guanidinato Complexes of Iridium: Ligand-Donor Strength, O_2 Reactivity, and (Alkene)peroxoiridium(III) Intermediates

Matthew R. Kelley and Jan-Uwe Rohde*

Department of Chemistry, The University of Iowa, Iowa City, Iowa 52242, United States

Supporting Information

ABSTRACT: A series of seven [Ir{ArNC(NR$_2$)NAr}(cod)] complexes (**1a**−**1g**; where R = Me or Et; Ar = Ph, 4-MeC$_6$H$_4$, 4-MeOC$_6$H$_4$, 2,6-Me$_2$C$_6$H$_3$, or 2,6-^{i}Pr$_2$C$_6$H$_3$; and cod = 1,5-cyclooctadiene) were synthesized by two different methods from the neutral guanidines, ArN=C(NR$_2$)NHAr, using either MeLi and [{Ir(cod)}$_2$(μ-Cl)$_2$] or [{Ir(cod)}$_2$(μ-OMe)$_2$]. Reaction of **1a**−**1g** with CO produced the corresponding [Ir{ArNC(NR$_2$)NAr}(CO)$_2$] complexes (**2a**−**2g**), which were characterized by NMR and solution- and solid-state IR spectroscopy. Complexes **1b** (R = Et, Ar = Ph), **1d** (R = Et, Ar = 4-MeC$_6$H$_4$), **1f** (R = Me, Ar = 2,6-Me$_2$C$_6$H$_3$), and **2b** (R = Et, Ar = Ph) were characterized by X-ray crystallography as mononuclear complexes with a guanidinato-κ^2N,N' ligand and a cod or two CO ligands coordinated to the Ir center in a distorted square-planar environment. On the basis of the CO stretching frequencies of **2a**−**2g** [avg. ν_{CO} (*n*-pentane) = 2016−2019 cm^{-1}] and the alkene ^{13}C chemical shifts of **1a**−**1g** [$\delta(^{13}C_{C=C})$ = 58.7−61.0 ppm], the donor strength of the guanidinato ligands was evaluated and compared to that of related monoanionic ligands. Reaction of **1a**−**1g** in solution with O_2 at 20 °C afforded (alkene)peroxoiridium(III) intermediates, [Ir{ArNC(NR$_2$)NAr}(cod)(O$_2$)] (**3**). The steric properties of the supporting ligand play a decisive role in O_2 binding in that complexes without ortho substituents react largely irreversibly with O_2 (**1a**−**1e**; where Ar = Ph, 4-MeC$_6$H$_4$ or 4-MeOC$_6$H$_4$), whereas complexes with ortho substituents exhibit fully reversible O_2 binding (**1f** and **1g**; where Ar = 2,6-Me$_2$C$_6$H$_3$ or 2,6-^{i}Pr$_2$C$_6$H$_3$). Complexes **3a**−**3f** were characterized by ^{1}H NMR and IR spectroscopy (ν_{OO} = 857−872 cm^{-1}). Decay of the new intermediates and subsequent reaction with cod produced 4-cycloocten-1-one and the respective Ir^I precursor.

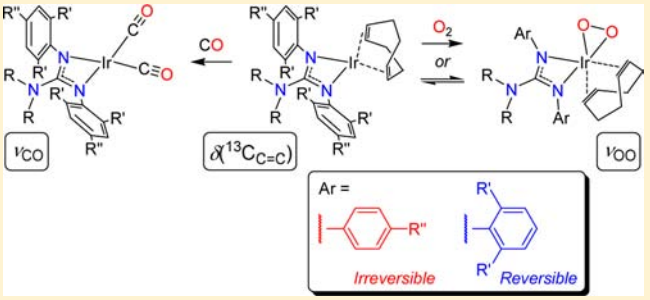

1. INTRODUCTION

Catalytic methods for the oxidation of organic compounds that use O_2 as oxidant offer significant economic and environmental advantages. Yet, the development of selective methods remains challenging.[1] While heterogeneous methods are effective for the bulk oxidation of selected substrates, homogeneous oxidation catalysis promises to be of broader synthetic utility.[2−4] In this context, organometallic O_2 reactivity is an area of growing interest,[5,6] because insights into this chemistry provide a basis for the design and development of catalytic methods that use O_2 or air. Complexes of Rh and Ir were extensively investigated in early studies on catalytic alkene oxidation.[7,8] These metals have received renewed attention in recent work focusing on stoichiometric O_2 reactions of well-defined alkene complexes.[9,10] In particular, the latter studies have led to the characterization of the products from C−O bond formation, such as metallaoxetanes and metalladioxolanes.[9−17]

By contrast, little is known about the mechanism of O_2 activation and how these products might form. In light of the abundance of peroxo complexes of Rh and Ir,[18,19] the intermediacy of (alkene)peroxo complexes en route to C−O bond formation has frequently been proposed.[7,10,11,14,20] A few such complexes have in fact been reported. These include [IrCl(PPh$_3$)$_2$(C$_2$H$_4$)(O$_2$)] and [Ir(phen)(cod)(O$_2$)]$^+$ (where cod = 1,5-cyclooctadiene), for which the presence of a peroxo ligand was confirmed by IR spectroscopy (ν_{OO} = 880 and 850 cm^{-1}).[21,22] Three other examples were characterized by X-ray crystallography, namely, a Rh^{III}(alkene)(O$_2^{2-}$) complex, in which the alkene group is part of a tridentate bis(phosphine) ligand,[23] and two Ir^{III}(C$_2$H$_4$)(O$_2^{2-}$) complexes supported by bis(pyridine)amine ligands.[24] Although vibrational data for ν_{OO} were not reported in these cases, the assignment of the O_2-derived ligand as a peroxo ligand could be based on the O−O distance. With one exception, the known (alkene)peroxo complexes did not exhibit the expected reactivity, however. Only for [IrCl(PPh$_3$)$_2$(C$_2$H$_4$)(O$_2$)] has oxidation of the ethene ligand to acetaldehyde been reported, but under concomitant oxidation of PPh$_3$ to OPPh$_3$.[25] No alkene oxygenation has been observed for the other (alkene)peroxo complexes.

With the goal of advancing mechanisms of O_2 activation, we have investigated the O_2 reactivity of Ir^I(alkene) complexes supported by monoanionic dialkyldiarylguanidinato ligands, {ArNC(NR$_2$)NAr}$^-$ (Chart 1).[26] Substituted guanidinates have been employed as ligands in a wide variety of transition metal complexes and, owing to their electronic properties, are well-

Received: November 27, 2012
Published: February 19, 2013

   dx.doi.org/10.1021/ic302570s | Inorg. Chem. 2013, 52, 2564−2580

Chart 1. Structures of Guanidines and Complexes 1−3

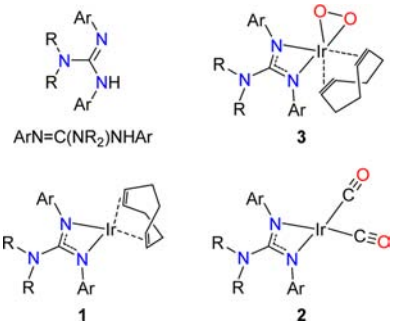

suited for the coordination of metals in mid and high oxidation states.[27−30] Only recently, guanidinato complexes of low-valent metal centers such as Ir^{I},[26,31,32] Rh^{I},[33] Co^{I},[34] and Ni^{I}[35] have emerged. In addition to these examples, guanidinato ligands have given access to a Cr^{I}_{2} complex[36] with a very short metal−metal distance and multinuclear Cu^{I}, Ag^{I}, and Au^{I} species[37] with short metal−metal contacts or interactions.

We found that [Ir{ArNC(NR$_2$)NAr}(cod)] complexes (**1**) react with O_2 under ambient conditions and reported the formation of an (alkene)peroxoiridium(III) intermediate, [Ir{PhNC(NMe$_2$)NPh}(cod)(O$_2$)] (**3a**), for one of these reactions.[38] Remarkably, this intermediate could be generated in high yield and persisted in solution for several hours, so that it could be characterized by spectroscopic techniques. Data for its decay products were consistent with the presence of an oxygenated cod ligand. Indeed, reactions with added alkenes (i.e., 1,5-cyclooctadiene or *cis*-cyclooctene) produced 4-cyclooctene-1-one, thus providing evidence for C−O bond formation. In following up on our initial findings, we have prepared an extended series of Ir^{I} complexes to examine electronic and steric substituent effects on the formation and properties of the new (alkene)peroxo intermediates (**3**). The results of this study are described in the present report. Furthermore, reactivity studies confirm the release of oxygenated alkene. We also report the synthesis and characterization of the dicarbonyl complexes [Ir{ArNC(NR$_2$)NAr}(CO)$_2$] (**2**) which were prepared for an evaluation of the donor strength of the guanidinato ligands.

2. EXPERIMENTAL SECTION

2.1. Materials and Methods. *Materials.* All reagents and solvents were purchased from commercial sources and were used as received, unless noted otherwise. Diethyl ether and toluene were deoxygenated by sparging with N_2 and purified by passage through two packed columns of molecular sieves under an N_2 pressure (MBraun solvent purification system). *n*-Pentane was dried over Na and distilled under N_2 prior to use.[39] Preparation and handling of air- and moisture-sensitive materials were carried out under an inert gas atmosphere by using either standard Schlenk and vacuum line techniques or a glovebox. Dioxygen was dried by passage through a short column of Drierite. The Ir complexes [{Ir(cod)}$_2$(μ-Cl)$_2$],[40] [Ir{PhNC(NMe$_2$)-NPh}(cod)] (**1a**), [Ir{PhNC(NEt$_2$)NPh}(cod)] (**1b**), [Ir{(4-MeC$_6$H$_4$)NC(NMe$_2$)N(4-MeC$_6$H$_4$)}(cod)] (**1c**), and [Ir{(2,6-Me$_2$C$_6$H$_3$)NC(NMe$_2$)N(2,6-Me$_2$C$_6$H$_3$)}(cod)] (**1f**) were synthesized according to published procedures (cod = 1,5-cyclooctadiene).[26] [{Ir(cod)}$_2$(μ-OMe)$_2$][41] was prepared from [{Ir(cod)}$_2$(μ-Cl)$_2$] and sodium methoxide[42] in dichloromethane, isolated by filtration and removal of the volatiles, and used without further purification. Elemental analyses were performed by Atlantic Microlab, Inc., Norcross, GA, U.S.A.

Physical Methods. NMR spectra were recorded on a Bruker Avance MicroBay 300, Avance DPX 300, Avance 400, or Avance 500 spectrometer at ambient temperature, unless noted otherwise. ^{1}H and ^{13}C chemical shifts are reported in parts per million (ppm) and were referenced to residual solvent peaks. Self-diffusion coefficients (D) were determined from stimulated-echo experiments[43] using bipolar gradients acquired in two-dimensional mode (stebpgp1s). These experiments were performed on a Bruker Avance 400 spectrometer at 25 °C. Prior to each experiment, the diffusion time (delay between the midpoints of the gradients, Δ) and gradient length (δ) were optimized using the one-dimensional version of the pulse sequence (stebpgp1s1d). The data acquisition for each diffusion experiment took approximately 30 min. Data processing and analysis to determine D were carried out within the TopSpin 2.1 software package.

IR spectra were recorded on a Bruker Vertex 70 Fourier-transform IR spectrometer using solutions of the compounds in *n*-pentane (5−15 mM) or solid samples. Solid samples were prepared by grinding the solid compound with KBr and pressing the mixture into a disk. Electrospray ionization mass spectral (ESI MS) data were acquired on a quadrupole ion trap ThermoFinnigan LCQ Deca mass spectrometer or on a quadrupole time-of-flight Waters Q-Tof Premier mass spectrometer. Electron impact ionization mass spectral (EI MS) data were acquired on a single quadrupole ThermoFinnigan Voyager mass spectrometer (equipped with a solids probe). UV−Visible spectra were recorded on an HP 8453A diode array spectrophotometer (Agilent Technologies), which was equipped with a cryostat from Unisoku Scientific Instruments, Japan, for measurements at low temperature.

2.2. Synthesis of Guanidines and Ir^{I} Complexes. *N,N-Diethyl-N′,N″-bis(4-methylphenyl)guanidine, (4-MeC$_6$H$_4$)N=C(NEt$_2$)NH(4-MeC$_6$H$_4$).* A solution of 2.00 g (7.80 mmol) of *N,N′*-bis(4-methylphenyl)thiourea and 4.90 mL (11.2 g, 78.7 mmol) of iodomethane in 15 mL of methanol was heated under reflux for 2 h. After the solution was cooled to room temperature, the volatiles, including excess iodomethane, were removed under reduced pressure to afford *S*-methyl-*N,N′*-bis(4-methylphenyl)isothiourea hydroiodide as a yellow solid. Yield: 3.00 g (97%). ^{1}H NMR (300 MHz, (CD$_3$)$_2$SO, δ): 10.81 (br, 2H, NH), 7.28 (br, 8H, Ar H), 2.65 (s, 3H, SCH$_3$), 2.32 (s, 6H, C$_6$H$_4$C*H*$_3$). ESI(+)MS (CH$_3$CN) *m/z*: {M − I}$^{+}$ calcd for C$_{16}$H$_{19}$IN$_2$S, 271.1; found, 271.2.

A solution of 3.00 g (7.53 mmol) of *S*-methyl-*N,N′*-bis(4-methylphenyl)isothiourea hydroiodide and 3.10 mL (2.19 g, 30.0 mmol) of diethylamine in 15 mL of methanol was heated in a sealed flask for 7 h at 70 °C. (***Caution!*** *Because of the formation of methanethiol, which is a gas under the reaction conditions, the pressure in the flask may increase substantially. A shield should be used for protection.*) The solution was cooled to room temperature, and methanethiol was carefully removed with a stream of N_2. (MeSH was trapped by routing the gas stream through concentrated HNO$_3$.) Upon evaporation of the solvents, *N,N*-diethyl-*N′,N″*-bis(4-methylphenyl)guanidinium iodide was obtained as a yellow solid. Yield: 3.05 g (96%). ^{1}H NMR (300 MHz, CDCl$_3$, δ): 7.12 (d, J = 8.6 Hz, 4H, Ar H), 7.02 (d, J = 8.4 Hz, 4H, Ar H), 5.49 (br, 2H, NH), 2.95 (q, J = 7.3 Hz, 4H, NC*H*$_2$CH$_3$), 2.32 (s, 3H, C$_6$H$_4$C*H*$_3$), 2.31 (s, 3H, C$_6$H$_4$C*H*$_3$), 1.40 (t, J = 7.3 Hz, 6H, NCH$_2$C*H*$_3$). ESI(+)MS (CH$_3$CN) *m/z*: {M − I}$^{+}$ calcd for C$_{19}$H$_{26}$IN$_3$, 296.2; found, 296.2.

A solution of 3.05 g (7.20 mmol) of *N,N*-diethyl-*N′,N″*-bis(4-methylphenyl)guanidinium iodide in 20 mL of diethyl ether was treated with 50 mL of a saturated aqueous solution of Na$_2$CO$_3$. The biphasic mixture was vigorously stirred for 1 h, after which the organic phase was separated and dried over MgSO$_4$ and the volatiles were removed under reduced pressure. The crude product was purified by column chromatography on silica gel using a solution of 3% NEt$_3$ in diethyl ether as the eluent affording a colorless solid. Yield: 1.45 g (68%). Anal. Calcd for C$_{19}$H$_{25}$N$_3$: C, 77.25; H, 8.53; N, 14.22. Found: C, 77.45; H, 8.52; N, 13.95. ^{1}H NMR (300 MHz, CDCl$_3$, δ): 7.04 (d, J = 8.0 Hz, 4H, Ar H), 6.80 (d, J = 7.5 Hz, 4H, Ar H), 5.35 (br, 1H, NH), 3.33 (q, J = 7.1 Hz, 4H, NC*H*$_2$CH$_3$), 2.29 (s, 6H, C$_6$H$_4$C*H*$_3$), 1.16 (t, J = 7.1 Hz, 6H, NCH$_2$C*H*$_3$). ^{13}C{^{1}H} NMR (75.5 MHz, CDCl$_3$, δ): 150.8, 131.4, 129.9, 122.2, and 118.7 (Ar), 42.1

dx.doi.org/10.1021/ic302570s | Inorg. Chem. 2013, 52, 2564−2580

(NCH_2CH_3), 20.8 ($C_6H_4CH_3$), 13.0 (NCH_2CH_3). EIMS (70 eV) *m/z*: $M^{+\bullet}$ calcd for $C_{19}H_{25}N_3$, 295.2; found, 295.3.

N,N′-Bis(4-methoxyphenyl)thiourea, (4-MeOC$_6$H$_4$NH)$_2$C═S. This compound[44] was synthesized using conditions reported for the synthesis of a closely related *N,N′*-diarylthiourea.[45] A solution of 1.12 mL (1.34 g, 7.95 mmol) of 4-methoxyphenyl isothiocyanate (98%) and 1.00 g (8.12 mmol) of 4-methoxyaniline in 10 mL of toluene was prepared and heated under reflux for 24 h, during which a purple solid was formed. The reaction mixture was cooled to room temperature, and the solid was separated by filtration, washed with cold toluene (3 × 5 mL) and dried in vacuo. Yield: 1.94 g (85%). ^{1}H NMR (300 MHz, $(CD_3)_2SO$, δ): 9.41 (s, 2H, NH), 7.30 (d, J = 8.9 Hz, 4H, Ar H), 6.88 (d, J = 8.9 Hz, 4H, Ar H), 3.73 (s, 6H, $C_6H_4OCH_3$). EIMS (70 eV) *m/z*: $M^{+\bullet}$ calcd for $C_{15}H_{16}N_2O_2S$, 288.1; found, 288.2.

N,N-Dimethyl-N′,N″-bis(4-methoxyphenyl)guanidine, (4-MeOC$_6$H$_4$)N═C(NMe$_2$)NH(4-MeOC$_6$H$_4$). A solution of 0.60 g (2.08 mmol) of *N,N′*-bis(4-methoxyphenyl)thiourea and 1.28 mL (2.92 g, 20.56 mmol) of iodomethane in 15 mL of methanol was heated under reflux for 2 h. After the solution was cooled to room temperature, the volatiles, including excess iodomethane, were removed under reduced pressure to afford *S*-methyl-*N,N′*-bis(4-methoxyphenyl)isothiourea hydroiodide as a yellow solid. Yield: 0.85 g (95%). ^{1}H NMR (300 MHz, $(CD_3)_2SO$, δ): 10.68 (br, 2H, NH), 7.33 (br, 4H, Ar H), 7.03 (br, 4H, Ar H), 3.77 (s, 6H, $C_6H_4OCH_3$), 2.66 (s, 3H, SCH_3). ESI(+)MS (CH_3CN) *m/z*: $\{M - I\}^+$ calcd for $C_{16}H_{19}IN_2O_2S$, 303.1; found, 303.1.

A solution of 0.75 g (1.74 mmol) of *S*-methyl-*N,N′*-bis(4-methoxyphenyl)isothiourea hydroiodide and 3.67 mL of a dimethylamine solution (5.6 M in EtOH; 20.55 mmol) in 15 mL of methanol was heated in a sealed flask for 7 h at 70 °C. (***Caution!*** *Because of the formation of methanethiol, which is a gas under the reaction conditions, the pressure in the flask may increase substantially. A shield should be used for protection.*) The solution was cooled to room temperature, and methanethiol was carefully removed with a stream of N_2. (MeSH was trapped by routing the gas stream through concentrated HNO_3.) Upon evaporation of the solvents, *N,N*-dimethyl-*N′,N″*-bis(4-methoxyphenyl)guanidinium iodide was obtained as a yellow solid. Yield: 0.68 g (91%). ^{1}H NMR (300 MHz, $(CD_3)_2SO$, δ): 9.28 (br, 2H, NH), 7.02 (d, J = 8.9 Hz, 4H, Ar H), 6.87 (d, J = 9.0 Hz, 4H, Ar H), 3.70 (s, 6H, $C_6H_4OCH_3$), 2.99 (s, 6H, NCH_3). ESI(+)MS (CH_3CN) *m/z*: $\{M - I\}^+$ calcd for $C_{17}H_{22}IN_3O_2$, 300.2; found, 300.2.

A solution of 0.45 g (1.05 mmol) of *N,N*-dimethyl-*N′,N″*-bis(4-methoxyphenyl)guanidinium iodide in 20 mL of diethyl ether was treated with 50 mL of a saturated aqueous solution of Na_2CO_3. The biphasic mixture was vigorously stirred for 1 h, after which the organic phase was separated and dried over $MgSO_4$ and the volatiles were removed under reduced pressure. The crude product was purified by column chromatography on silica gel using a solution of 5% NEt_3 in diethyl ether as the eluent affording an off-white solid. Yield: 0.15 g (47%). Anal. Calcd for $C_{17}H_{21}N_3O_2$: C, 68.20; H, 7.07; N, 14.04. Found: C, 67.73; H, 7.11; N, 13.75. ^{1}H NMR (300 MHz, $CDCl_3$, δ): 6.84−6.76 (m, 8H, Ar H), 4.82 (br, 1H, NH), 3.74 (s, 6H, $C_6H_4OCH_3$), 2.83 (s, 6H, NCH_3). ^{13}C{^{1}H} NMR (75.5 MHz, $CDCl_3$, δ): 155.2, 153.0, 122.1, and 114.8 (Ar), 55.6 ($C_6H_4OCH_3$), 38.3 (NCH_3). EIMS (70 eV) *m/z*: $M^{+\bullet}$ calcd for $C_{17}H_{21}N_3O_2$, 299.2; found, 299.4.

*General Procedure for the Synthesis of [Ir{ArNC(NR$_2$)NAr}(cod)] Complexes **1a**−**1f**.* **Method A.** In a typical procedure, 1.20 mmol of the *N,N*-dialkyl-*N′,N″*-diarylguanidine was dissolved in 15 mL of degassed diethyl ether. The solution was cooled to −40 °C and 1.1 equiv of methyllithium (1.6 M in Et_2O) was added under stirring. The resulting solution was allowed to warm to 20 °C and stirred for 1 h. Upon removal of the volatiles under reduced pressure, the Li^+ salt of the *N,N*-dialkyl-*N′,N″*-diarylguanidinate anion, Li{ArNC(NR$_2$)NAr}·Et_2O, was isolated as a colorless powder and stored under rigorous exclusion of moisture. The powder could also be recrystallized from a concentrated *n*-pentane solution at −30 °C to afford a microcrystalline solid.

In an N_2 atmosphere, a solution of 0.300 mmol of lithium guanidinate in 10 mL of diethyl ether was added to a suspension of 100 mg (0.149 mmol) of $[\{Ir(cod)\}_2(\mu\text{-}Cl)_2]$ in 5 mL of diethyl ether under stirring at 20 °C. The color of the reaction mixture changed from orange to yellow, accompanied by precipitation of a colorless solid. After 3 h, the solution was filtered, and the solvent was removed under reduced pressure. The residue was recrystallized from *n*-pentane by preparing a concentrated solution at 20 °C and storing it at −30 °C. Yellow single crystals of X-ray diffraction quality were typically obtained within 2 days.

Method B. In an N_2 atmosphere, a solution of 0.300 mmol of the *N,N*-dialkyl-*N′,N″*-diarylguanidine in 15 mL of diethyl ether was added to a suspension of 0.149 mmol of $[\{Ir(cod)\}_2(\mu\text{-}OMe)_2]$ in 5 mL of diethyl ether under stirring. The dark-orange mixture turned into a yellow-orange solution. After 3 h, the volatiles were removed under reduced pressure to afford a yellow-orange oil. The residue was recrystallized as described above (Method A).

*[Ir{(4-MeC$_6$H$_4$)NC(NMe$_2$)N(4-MeC$_6$H$_4$)}(cod)] (**1c**).* The synthesis and characterization of this compound were described previously, but the new UV−Vis data differ slightly from those reported earlier.[26,46] UV−Vis (toluene) λ_{max}, nm (ε): 370 (sh), 418 (1700), 470 (300). All other characterization data, which were obtained from the same batch as used for UV−Vis spectroscopy, were indistinguishable from the reported data.

*[Ir{(4-MeC$_6$H$_4$)NC(NEt$_2$)N(4-MeC$_6$H$_4$)}(cod)] (**1d**).* Yield (Method A): 114 mg (64%). Anal. Calcd for $C_{27}H_{36}IrN_3$: C, 54.52; H, 6.10; N, 7.06. Found: C, 54.81; H, 6.01; N, 7.02. ^{1}H NMR (300 MHz, $CDCl_3$, δ): 7.00 (d, J = 8.6 Hz, 4H, Ar H), 6.72 (d, J = 8.2 Hz, 4H, Ar H), 3.60 (br m, 4H, =C*H*CH_2−), 2.86 (q, J = 7.1 Hz, 4H, NCH_2CH_3), 2.29 (s, 6H, $C_6H_4CH_3$), 2.18 (br m, 4H, =CHCH_2−), 1.43 (m, 4H, =CHCH_2−), 1.02 (t, J = 7.1 Hz, 6H, NCH_2CH_3). ^{13}C{^{1}H} NMR (75.5 MHz, $CDCl_3$, δ): 145.2, 131.1, 129.2, and 121.8 (Ar), 60.7 (=CHCH_2−), 41.0 (NCH_2CH_3), 31.8 (=CHCH_2−), 20.8 ($C_6H_4CH_3$), 12.0 (NCH_2CH_3). EIMS (70 eV) *m/z*: $M^{+\bullet}$ calcd for $C_{27}H_{36}IrN_3$, 595.3; found, 595.2. UV−Vis (toluene) λ_{max}, nm (ε): 370 (sh), 419 (1700), 471 (300). This complex was also synthesized using Method B. Yield: 58%. The UV−Vis spectrum of this batch was identical to that of the product obtained from Method A.

*[Ir{(4-MeOC$_6$H$_4$)NC(NMe$_2$)N(4-MeOC$_6$H$_4$)}(cod)] (**1e**).* Yield (Method B): 116 mg (65%). Anal. Calcd for $C_{25}H_{32}IrN_3O_2$: C, 50.15; H, 5.39; N, 7.02. Found: C, 50.40; H, 5.58; N, 6.94. ^{1}H NMR (300 MHz, $CDCl_3$, δ): 6.79−6.71 (m, 8H, Ar H), 3.77 (s, 6H, $C_6H_4OCH_3$), 3.63 (br m, 4H, =C*H*CH_2−), 2.49 (s, 6H, NCH_3), 2.19 (br m, 4H, =CHCH_2−), 1.44 (m, 4H, =CHCH_2−). ^{13}C{^{1}H} NMR (75.5 MHz, $CDCl_3$, δ): 174.5 (CN_3), 154.7, 140.8, 123.3, and 113.9 (Ar), 60.7 (=CHCH_2−), 55.4 ($C_6H_4OCH_3$), 38.9 (NCH_3), 31.8 (=CHCH_2−). EIMS (70 eV) *m/z*: $M^{+\bullet}$ calcd for $C_{25}H_{32}IrN_3O_2$, 599.2; found, 599.2. UV−Vis (toluene) λ_{max}, nm (ε): 370 (sh), 419 (1600), 471 (300).

*[Ir{(2,6-^{i}Pr$_2$C$_6$H$_3$)NC(NMe$_2$)N(2,6-^{i}Pr$_2$C$_6$H$_3$)}(cod)] (**1g**).* This compound was synthesized from Li{(2,6-^{i}Pr$_2$C$_6$H$_3$)NC(NMe$_2$)N-(2,6-^{i}Pr$_2$C$_6$H$_3$)} (prepared in situ as described elsewhere[36,47]) and $[\{Ir(cod)\}_2(\mu\text{-}Cl)_2]$ according to the general procedure described above (Method A). Yield: 110 mg (52%). Anal. Calcd for $C_{35}H_{52}IrN_3$: C, 59.46; H, 7.41; N, 5.94. Found: C, 59.88; H, 7.30; N, 6.14. ^{1}H NMR (300 MHz, $CDCl_3$, δ): 7.09−6.98 (m, 6H, Ar H), 3.77 (sept, J = 6.8 Hz, 4H, Ar C*H*$(CH_3)_2$), 3.36 (br m, 4H, =C*H*CH_2−), 2.23 (s, 6H, NCH_3), 2.04 (br m, 4H, =CHCH_2−), 1.37 (d, J = 6.8 Hz, 12H, Ar CH$(CH_3)_2$), 1.32 (m, 4H, =CHCH_2−), 1.21 (d, J = 6.9 Hz, 12H, Ar CH$(CH_3)_2$). ^{13}C{^{1}H} NMR (75.5 MHz, $CDCl_3$, δ): 175.4 (CN_3), 143.9, 141.7, 124.0, and 123.1 (Ar), 58.7 (=CHCH_2−), 38.5 (NCH_3), 31.8 (=CHCH_2−), 27.1 (Ar CH$(CH_3)_2$), 25.3 and 23.4 (Ar CH$(CH_3)_2$). EIMS (70 eV) *m/z*: $M^{+\bullet}$ calcd for $C_{35}H_{52}IrN_3$, 707.4; found, 707.6. UV−Vis (toluene) λ_{max}, nm (ε): 370 (900), 423 (900), 476 (300).

*[Ir{PhNC(NMe$_2$)NPh}(CO)$_2$] (**2a**).* A steady stream of CO(*g*) was purged through a solution of 100 mg (0.186 mmol) of [Ir{PhNC-(NMe$_2$)NPh}(cod)] in 15 mL of diethyl ether for 15 min at 20 °C. The yellow solution gradually turned purple over the first 5 min. Subsequently, the volatiles were removed under reduced pressure to afford a purple solid. Because of the low solubility of the solid in *n*-

dx.doi.org/10.1021/ic302570s | Inorg. Chem. 2013, 52, 2564−2580

pentane, the preparation of a saturated solution suitable for growing single crystals required about a day. After separation of undissolved solid, the solution was stored at −30 °C. Formation of yellow single crystals typically occurred within 2 days. Yield: 61 mg (68%). Anal. Calcd for $C_{17}H_{16}IrN_3O_2$: C, 41.97; H, 3.31; N, 8.64. Found: C, 42.09; H, 3.20; N, 8.59. ^{1}H NMR (300 MHz, C_6D_6, δ): 7.06 (t, J = 8.1 Hz, 4H, Ar H), 6.85 (d, J = 8.1 Hz, 4H, Ar H), 6.81 (t, J = 7.3 Hz, 2H, Ar H), 1.82 (s, 6H, NCH_3). $^{13}C\{^1H\}$ NMR (75.5 MHz, C_6D_6, δ): 175.6 (IrCO), 171.1 (CN_3), 148.2, 129.3, 123.3, and 123.0 (Ar), 38.0 (NCH_3). EIMS (70 eV) m/z: $M^{+\bullet}$ calcd for $C_{17}H_{16}IrN_3O_2$, 487.1; found, 487.1. IR (n-pentane, cm^{-1}): 2055 and 1983 (ν_{CO}). IR (KBr, cm^{-1}): 2042 and 1956 (ν_{CO}). UV−Vis (toluene) λ_{max}, nm: 355 (sh). It should be noted that solutions of **2a** in n-pentane, benzene-d_6, and diethyl ether slowly turned pink upon standing for several hours. No changes, however, were observed in the IR (n-C_5H_{12}, C_6D_6 and Et_2O) and ^{1}H NMR spectra (C_6D_6) of these solutions. Upon standing at 20 °C, **2a** was recovered from the n-pentane solution as a yellow microcrystalline solid.

*Synthesis and Characterization of [Ir{ArNC(NR$_2$)NAr}(CO)$_2$] Complexes **2b**−**2g**.* The iridium dicarbonyls **2b**−**2g** were synthesized in a manner analogous to **2a**. The reaction solutions turned purple (**2b** and **2c**), yellow-orange (**2d**, **2f**, and **2g**) or green (**2e**) over a similar time frame as observed for **2a**. Between 50 and 100 mg of the Ir^I(cod) complexes was used, and the corresponding Ir^I(CO)$_2$ complexes were obtained as yellow solids in yields of 65−80% (**2b**−**2f**, after recrystallization) and 48% (**2g**).

*[Ir{PhNC(NEt$_2$)NPh}(CO)$_2$] (**2b**).* Anal. Calcd for $C_{19}H_{20}IrN_3O_2$: C, 44.35; H, 3.92; N, 8.17. Found: C, 44.64; H, 3.87; N, 8.20. ^{1}H NMR (300 MHz, C_6D_6, δ): 7.11−7.01 (m, 8H, Ar H), 6.82 (t, J = 7.1 Hz, 2H, Ar H), 2.45 (q, J = 7.2 Hz, 4H, NCH_2CH_3), 0.43 (t, J = 7.2 Hz, 6H, NCH_2CH_3). EIMS (70 eV) m/z: $M^{+\bullet}$ calcd for $C_{19}H_{20}IrN_3O_2$, 515.1; found, 515.2. IR (n-pentane, cm^{-1}): 2055 and 1982 (ν_{CO}). IR (KBr, cm^{-1}): 2051 and 1963 (ν_{CO}). UV−Vis (toluene) λ_{max}, nm: 355 (sh).

*[Ir{(4-MeC$_6$H$_4$)NC(NMe$_2$)N(4-MeC$_6$H$_4$)}(CO)$_2$] (**2c**).* Anal. Calcd for $C_{19}H_{20}IrN_3O_2$: C, 44.35; H, 3.92; N, 8.17. Found: C, 44.28; H, 3.87; N, 8.08. ^{1}H NMR (300 MHz, C_6D_6, δ): 6.90 (d, J = 8.1 Hz, 4H, Ar H), 6.82 (d, J = 8.5 Hz, 4H, Ar H), 2.11 (s, 6H, $C_6H_4CH_3$), 1.89 (s, 6H, NCH_3). EIMS (70 eV) m/z: $M^{+\bullet}$ calcd for $C_{19}H_{20}IrN_3O_2$, 515.1; found, 515.1. IR (n-pentane, cm^{-1}): 2054 and 1981 (ν_{CO}). IR (KBr, cm^{-1}): 2044 and 1970 (ν_{CO}). UV−Vis (toluene) λ_{max}, nm: 355 (sh).

*[Ir{(4-MeC$_6$H$_4$)NC(NEt$_2$)N(4-MeC$_6$H$_4$)}(CO)$_2$] (**2d**).* Anal. Calcd for $C_{21}H_{24}IrN_3O_2$: C, 46.48; H, 4.46; N, 7.74. Found: C, 46.48; H, 4.52; N, 7.69. ^{1}H NMR (300 MHz, C_6D_6, δ): 6.98 (d, J = 8.4 Hz, 4H, Ar H), 6.89 (d, J = 8.0 Hz, 4H, Ar H), 2.52 (q, J = 7.1 Hz, 4H, NCH_2CH_3), 2.10 (s, 6H, $C_6H_4CH_3$), 0.49 (t, J = 7.1 Hz, 6H, NCH_2CH_3). EIMS (70 eV) m/z: $M^{+\bullet}$ calcd for $C_{21}H_{24}IrN_3O_2$, 543.2; found, 543.3. IR (n-pentane, cm^{-1}): 2053 and 1980 (ν_{CO}). IR (KBr, cm^{-1}): 2053 and 1958 (ν_{CO}). UV−Vis (toluene) λ_{max}, nm: 355 (sh).

*[Ir{(4-MeOC$_6$H$_4$)NC(NMe$_2$)N(4-MeOC$_6$H$_4$)}(CO)$_2$] (**2e**).* Anal. Calcd for $C_{20}H_{22.5}IrN_3O_{4.25}$ (**2e**·0.25Et$_2$O): C, 42.51; H, 4.01; N, 7.44. Found: C, 42.31; H, 3.73; N, 7.54. ^{1}H NMR (300 MHz, C_6D_6, δ): 6.82 (d, J = 9.0 Hz, 4H, Ar H), 6.69 (d, J = 9.0 Hz, 4H, Ar H), 3.32 (s, 6H, $C_6H_4OCH_3$), 1.93 (s, 6H, NCH_3). EIMS (70 eV) m/z: $M^{+\bullet}$ calcd for $C_{19}H_{20}IrN_3O_4$, 547.1; found, 547.3. IR (n-pentane, cm^{-1}): 2053 and 1980 (ν_{CO}). IR (KBr, cm^{-1}): 2041 and 1962 (ν_{CO}). UV−Vis (toluene) λ_{max}, nm: 355 (sh).

*[Ir{(2,6-Me$_2$C$_6$H$_3$)NC(NMe$_2$)N(2,6-Me$_2$C$_6$H$_3$)}(CO)$_2$] (**2f**).* Anal. Calcd for $C_{21}H_{24}IrN_3O_2$: C, 46.48; H, 4.46; N, 7.74. Found: C, 46.63; H, 4.40; N, 7.68. ^{1}H NMR (300 MHz, C_6D_6, δ): 6.93 (d, J = 7.8 Hz, 4H, Ar H), 6.85 and 6.83 (dd, J = 6.7 Hz, J = 8.5 Hz, 2H, Ar H), 2.40 (s, 12H, $C_6H_3(CH_3)_2$), 1.69 (s, 6H, NCH_3). EIMS (70 eV) m/z: $M^{+\bullet}$ calcd for $C_{21}H_{24}IrN_3O_2$, 543.2; found, 543.3. IR (n-pentane, cm^{-1}): 2053 and 1980 (ν_{CO}). IR (KBr, cm^{-1}): 2044 and 1977 (ν_{CO}). UV−Vis (toluene) λ_{max}, nm (ε): 353 (2400), 380 (sh), 410 (sh).

*[Ir{(2,6-^{i}Pr$_2$C$_6$H$_3$)NC(NMe$_2$)N(2,6-^{i}Pr$_2$C$_6$H$_3$)}(CO)$_2$] (**2g**).* Anal. Calcd for $C_{29}H_{40}IrN_3O_2$: C, 53.19; H, 6.16; N, 6.42. Found: C, 53.39; H, 6.27; N, 6.41. ^{1}H NMR (300 MHz, C_6D_6, δ): 7.06−7.03 (m, 6H, Ar H), 3.85 (sept, J = 6.8 Hz, 4H, Ar $CH(CH_3)_2$), 1.88 (s, 6H, NCH_3), 1.46 (d, J = 6.8 Hz, 12H, Ar $CH(CH_3)_2$), 1.21 (d, J = 6.9 Hz, 12H, Ar $CH(CH_3)_2$). EIMS (70 eV) m/z: $M^{+\bullet}$ calcd for $C_{29}H_{40}IrN_3O_2$, 655.3; found, 655.5. IR (n-pentane, cm^{-1}): 2052 and 1980 (ν_{CO}). IR (KBr, cm^{-1}): 2044 and 1966 (ν_{CO}). UV−Vis (toluene) λ_{max}, nm (ε): 353 (2300), 380 (sh), 410 (sh).

2.3. Generation and Reactivity of Ir^{III} Complexes. *Reactions of **1a**−**1g** with O_2.* A 2 mM solution of [Ir{ArNC(NR$_2$)NAr}(cod)] (**1a**−**1g**, 0.002 mmol) in 1 mL of toluene was placed in a 0.5-cm UV−Vis cuvette and precooled to 0 °C. The solution was purged with O_2(g) for 40 s and kept under an O_2 atmosphere. The half-lives of the reactions were determined by UV−Vis spectroscopy, and the reported values represent averages of three runs. The reaction of **1a** with O_2 was also investigated using a single-wavelength spectrophotometer (λ = 419 nm) with minimal exposure time and under protection from ambient light, showing that the half-life was not affected by light from the UV lamp of the instrument or by ambient light.

To investigate reversibility, the reaction of 2 mM **1f** (0.002 mmol) in 1 mL of toluene with O_2 at 20 °C was monitored by UV−Vis spectroscopy until the decay of **1f** leveled off (ca. 2 h). The solution was then purged with Ar for 1 min to remove O_2, after which the regeneration of **1f** was monitored.

*Generation and Characterization of [Ir{ArNC(NR$_2$)NAr}(η^4-cod)-(η^2-O$_2$)] Complexes **3b**−**3f**.* Complexes **3b**−**3f** were generated as recently described for [Ir{PhNC(NMe$_2$)NPh}(η^4-cod)(η^2-O$_2$)] (**3a**).[38] In a typical experiment, a 15−20 mM solution of **1b**−**1f** (0.0075−0.010 mmol) in 0.5 mL of C_6D_6 was placed in an NMR tube, purged with O_2(g) at 20 °C for 40 s, and kept under an O_2 atmosphere for the remainder of the reaction. The progress of the reaction was monitored by ^{1}H NMR spectroscopy. Under these conditions, **1b**−**1e** (bright yellow solutions) converted into the corresponding intermediates, **3b**−**3e** (pale yellow solutions), in about 2−3 h, and the intermediates were typically decayed (dark green solutions) within 20 h after the addition of O_2 to **1b**−**1e**. Reversible formation of **3f** reached its maximum within half a day (ca. 60% relative to 1,2-dichloroethane added as a standard). For IR spectroscopy, 0.15 mL of a solution of **3b**−**3f** was mixed with KBr. The mixture was evaporated to dryness (20 °C, in vacuo) and pressed into a disk.

*[Ir{PhNC(NEt$_2$)NPh}(η^4-cod)(η^2-O$_2$)] (**3b**).* ^{1}H NMR (300 MHz, C_6D_6, δ): 7.44 (d, J = 7.3 Hz, 4H, Ar H), 7.18−7.09 (m, Ar H; these signals partially overlap with the residual solvent peak), 6.96 (t, J = 7.4 Hz, 1H, Ar H), 6.89 (t, J = 7.3 Hz, 1H, Ar H), 4.76−4.67 (br m, 1H, =CHCH$_2$−), 4.55−4.46 (br m, 1H, =CHCH$_2$−), 4.18−4.00 (br m, 2H, =CHCH$_2$−), 2.83 (m, 2H, NCH_2CH_3), 2.39−1.86 (br m, 6H, =CHCH_2−), 2.33 (m, 2H, NCH_2CH_3), 1.71−1.55 (br m, 2H, =CHCH_2−), 0.62 (dd, J = 7.1 Hz, J = 7.1 Hz, 6H, NCH_2CH_3). IR (KBr, cm^{-1}): 865 (ν_{OO}), 576 and 459 (ν_{IrO}).

*[Ir{(4-MeC$_6$H$_4$)NC(NMe$_2$)N(4-MeC$_6$H$_4$)}(η^4-cod)(η^2-O$_2$)] (**3c**).* ^{1}H NMR (300 MHz, C_6D_6, δ): 7.30 (d, J = 7.9 Hz, 2H, Ar H), 7.25 (d, J = 8.3 Hz, 2H, Ar H), 6.98 (d, J = 7.9 Hz, 2H, Ar H), 6.93 (d, J = 8.0 Hz, 2H, Ar H), 4.80−4.70 (br m, 1H, =CHCH$_2$−), 4.64−4.53 (br m, 1H, =CHCH$_2$−), 4.20−4.10 (br m, 1H, =CHCH$_2$−), 4.10−4.00 (br m, 1H, =CHCH$_2$−), 2.42−1.95 (br m, 6H, =CHCH_2−), 2.12 (s, 3H, $C_6H_4CH_3$), 2.11 (s, 3H, $C_6H_4CH_3$), 2.09 (s, 6H, NCH_3), 1.77−1.58 (br m, 2H, =CHCH_2−). IR (KBr, cm^{-1}): 862 (ν_{OO}), 575 and 459 (ν_{IrO}).

*[Ir{(4-MeC$_6$H$_4$)NC(NEt$_2$)N(4-MeC$_6$H$_4$)}(η^4-cod)(η^2-O$_2$)] (**3d**).* ^{1}H NMR (300 MHz, C_6D_6, δ): 7.38 (d, J = 8.3 Hz, 4H, Ar H), 6.99 (d, J = 8.4 Hz, 2H, Ar H), 6.95 (d, J = 8.1 Hz, 2H, Ar H), 4.78−4.72 (br m, 1H, =CHCH$_2$−), 4.61−4.53 (br m, 1H, =CHCH$_2$−), 4.20−4.06 (br m, 2H, =CHCH$_2$−), 2.91 (m, 2H, NCH_2CH_3), 2.38 (m, 2H, NCH_2CH_3), 2.30−1.96 (br m, 6H, =CHCH_2−), 2.11 (s, 3H, $C_6H_4CH_3$), 2.10 (s, 3H, $C_6H_4CH_3$), 1.76−1.61 (br m, 2H, =CHCH_2−), 0.67 (dd, J = 7.1 Hz, J = 7.1 Hz, 6H, NCH_2CH_3). IR (KBr, cm^{-1}): 862 (ν_{OO}), 575 and 458 (ν_{IrO}).

*[Ir{(4-MeOC$_6$H$_4$)NC(NMe$_2$)N(4-MeOC$_6$H$_4$)}(η^4-cod)(η^2-O$_2$)] (**3e**).* ^{1}H NMR (300 MHz, C_6D_6, δ): 7.32 (d, J = 8.8 Hz, 2H, Ar H), 7.26 (d, J = 8.6 Hz, 2H, Ar H), 6.78 (d, J = 8.9 Hz, 2H, Ar H), 6.73 (d, J = 8.7 Hz, 2H, Ar H), 4.78−4.67 (br m, 1H, =CHCH$_2$−), 4.66−4.58 (br m, 1H, =CHCH$_2$−), 4.22−4.13 (br m, 1H, =CHCH$_2$−), 4.08−3.99 (br m, 1H, =CHCH$_2$−), 3.34 (s, 3H, $C_6H_4OCH_3$), 3.32 (s, 3H, $C_6H_4OCH_3$), 2.40−2.15 (br m, 4H, =CHCH_2−), 2.15−1.97 (br m, 2H,

dx.doi.org/10.1021/ic302570s | Inorg. Chem. 2013, 52, 2564−2580

Table 1. Crystallographic Data and Structure Refinement Parameters for 1b, 1d, 1f, and 2b[a]

	1b	1d	1f	2b
empirical formula	$C_{25}H_{32}IrN_3$	$C_{27}H_{36}IrN_3$	$C_{27}H_{36}IrN_3$	$C_{19}H_{20}IrN_3O_2$
formula weight	566.74	594.79	594.79	514.58
temperature, T	209(2) K	210(2) K	190(2) K	190(2) K
wavelength, λ	0.71073 Å	0.71073 Å	0.71073 Å	0.71073 Å
crystal system	monoclinic	triclinic	monoclinic	tetragonal
space group	$P2_1/n$	$P\bar{1}$	$P2_1/c$	$P\bar{4}n2$
unit cell dimensions	a = 10.2528(11) Å	a = 9.5336(11) Å	a = 15.1915(16) Å	a = 17.3359(18) Å
	b = 17.8077(19) Å	b = 9.6634(11) Å	b = 7.6661(9) Å	
	c = 12.6997(14) Å	c = 13.6109(15) Å	c = 20.783(3) Å	c = 6.1770(7) Å
		α = 87.444(5)°		
	β = 107.034(5)°	β = 89.343(5)°	β = 94.776(5)°	
		γ = 74.719(5)°		
volume, V	2217.0(4) Å^3	1208.4(2) Å^3	2412.0(5) Å^3	1856.4(3) Å^3
Z	4	2	4	4
calculated density	1.698 Mg·m^{-3}	1.635 Mg·m^{-3}	1.638 Mg·m^{-3}	1.841 Mg·m^{-3}
absorption coefficient, μ	6.038 mm^{-1}	5.543 mm^{-1}	5.554 mm^{-1}	7.209 mm^{-1}
reflections collected	19485	10816	19363	11591
independent reflections[b]	5287 (R_{int} = 0.0388)	5740 (R_{int} = 0.0166)	5510 (R_{int} = 0.0369)	2215 (R_{int} = 0.0253)
reflections with $I > 2\sigma(I)$	4310	5298	4630	2052
data/restraints/parameters	5287/4/276	5740/4/296	5510/4/298	2215/0/117
goodness-of-fit on F^2[c]	1.035	1.118	1.029	1.210
final R indices $[I > 2\sigma(I)]$[d,e]	$R1$ = 0.0246,	$R1$ = 0.0225,	$R1$ = 0.0224,	$R1$ = 0.0275,
	$wR2$ = 0.0472	$wR2$ = 0.0516	$wR2$ = 0.0437	$wR2$ = 0.0857
R indices (all data)[d,e]	$R1$ = 0.0371,	$R1$ = 0.0264,	$R1$ = 0.0332,	$R1$ = 0.0308,
	$wR2$ = 0.0505	$wR2$ = 0.0531	$wR2$ = 0.0468	$wR2$ = 0.0873
absolute structure parameter				0.08(2)
largest diff. peak and hole	0.922 and −0.707 e·A^{-3}	1.108 and −1.175 e·A^{-3}	1.386 and −0.775 e·A^{-3}	1.281 and −0.571 e·A^{-3}

[a]Data for **1b** and **1f** taken from structures reported in ref 26. [b]$R_{int} = \sum|F_o^2 - \langle F_o^2\rangle|/\sum[F_o^2]$. [c]GOF = $S = \{\sum[w(F_o^2 - F_c^2)^2]/(n-p)\}^{1/2}$. [d]$R1 = \sum||F_o| - |F_c||/\sum|F_o|$. [e]$wR2 = \{\sum[w(F_o^2 - F_c^2)^2]/\sum[w(F_o^2)^2]\}^{1/2}$, where $w = 1/[\sigma^2(F_o^2) + (aP)^2 + bP]$ and $P = (F_o^2 + 2F_c^2)/3$.

=CHCH_2−), 2.12 (s, 6H, NCH_3), 1.82−1.57 (br m, 2H, =CHCH_2−). IR (KBr, cm^{-1}): 857 (ν_{OO}), 573 and 457 (ν_{IrO}).

*[Ir{(2,6-Me$_2$C$_6$H$_3$)NC(NMe$_2$)N(2,6-Me$_2$C$_6$H$_3$)}(η^4-cod)(η^2-O$_2$)] (**3f**).* ^{1}H NMR (300 MHz, C_6D_6, δ): 7.04−6.83 (Ar H, **3f** and **1f**), 5.25−5.17 (br m, 1H, =C*H*CH$_2$−, **3f**), 4.79−4.69 (br m, 2H, =C*H*CH$_2$−, **3f**), 4.08−3.98 (br m, 1H, =C*H*CH$_2$−, **3f**), 3.59 (br m, 4H, =C*H*CH$_2$−, **1f**), 2.90 (s, 3H, C$_6$H$_3$(CH_3)$_2$, **3f**), 2.64 (s, 3H, C$_6$H$_3$(CH_3)$_2$, **3f**), 2.57 (s, 12H, C$_6$H$_3$(CH_3)$_2$, **1f**), 2.5−1.0 (=CHCH_2−, **3f** and **1f**), 2.22 (s, 3H, C$_6$H$_3$(CH_3)$_2$, **3f**), 2.18 (s, 3H, C$_6$H$_3$(CH_3)$_2$, **3f**), 1.89 (s, 6H, NCH_3, **3f**), 1.83 (s, 6H, NCH_3, **1f**). IR (KBr, cm^{-1}): 872 (ν_{OO}), 572 and 459 (ν_{IrO}).

*Reaction of **3a** with CO.* A solution of **3a** in C_6D_6 was prepared as previously described (ca. 3 h for the formation of **3a**),[38] then purged with CO(*g*) for 10 min and kept under a CO atmosphere at 20 °C for 1 d. Complex **2a** (IR, ^{1}H NMR), free cod (^{1}H NMR), and [Ir{PhNC(NMe$_2$)NPh}(cod)(CO$_3$)] (**4a**, ESI MS, IR) were identified as products. Quantification of **2a** and cod was carried out against 1,2-dichloroethane (δ, 2.90 ppm) as a standard, using the NMe$_2$ (**2a**) and alkene (cod) proton signals. ^{1}H NMR (300 MHz, C_6D_6, δ): 7.07 (m, Ar H, **2a**), 6.89−6.78 (m, Ar H, **2a**), 5.57 (br m, 4H, =C*H*CH$_2$−, free cod), 2.20 (br m, 8H, =CHCH_2−, free cod), 1.79 (s, 6H, NCH_3, **2a**). ESI(+)MS (*m*/*z*): {**4a** + H}$^+$ calcd for $C_{24}H_{28}IrN_3O_3$, 600.2; found, 538.2 ({**4a** − HCO$_3$}$^+$), 554.2 ({**3a** − OH}$^+$), 570.2 ({**3a** − H}$^+$), 600.2 ({**4a** + H}$^+$), 622.2 ({**4a** + Na}$^+$). IR (KBr, cm^{-1}): 2046 (ν_{CO}, **2a**), 2020 (ν_{CO}), 1969 (ν_{CO}, **2a**), 1690 (ν_{CO}, **4a**). For **3a**-^{18}O$_2$ + CO, ESI(+)MS (*m*/*z*): 538.2 ({**4a** − HCO$_3$}$^+$), 556.2 ({**3a** − OH}$^+$), 574.2 ({**3a** − H}$^+$), 604.2 ({**4a** + H}$^+$), 626.2 ({**4a** + Na}$^+$). IR (KBr, cm^{-1}): 2046 (ν_{CO}, **2a**), 2014 (ν_{CO}), 1969 (ν_{CO}, **2a**), 1690 (ν_{CO}, **4a**), 1667 (ν_{CO}, **4a**).

*Recovery of N,N-Dimethyl-N′,N″-diphenylguanidine, PhN═C(NMe$_2$)NHPh, from the Decay Products of **3a**.* A solution of 9.8 mg (0.018 mmol) of **1a** in 3 mL of toluene was purged with O_2 (40 s) at 20 °C. After 16 h, 3.0 μL (3.6 mg, 0.036 mmol) of concentrated HCl and 3 mL of water were added to the resulting green solution. The biphasic mixture was vigorously stirred for 1 h. The aqueous phase was separated and combined with 5 mL of diethyl ether and 15 mL of a saturated Na_2CO_3 solution. The biphasic mixture was vigorously stirred for 1 h, after which the organic phase was separated and dried over $MgSO_4$ and the volatiles were removed under reduced pressure. Yield: 2.9 mg (67%). The ^{1}H NMR and ESI(+)MS data were indistinguishable from those of the guanidine ligand precursor[26] and did not reveal any other products. ^{1}H NMR (300 MHz, $CDCl_3$, δ): 7.20 (t, J = 6.8 Hz, 4H, Ar H), 7.01 (t, J = 7.4 Hz, 2H, Ar H), 6.92 (d, J = 7.6 Hz, 4H, Ar H), 2.86 (s, 6H, NCH_3). ESI(+)MS (CH_3CN) *m*/*z*: {M + H}$^+$ calcd for $C_{15}H_{17}N_3$, 240.2; found, 240.2.

2.4. X-ray Crystallographic Analyses. A single crystal of each compound was coated with Paratone N oil and mounted on a glass capillary for data collection at 210(2) or 190(2) K on a Nonius KappaCCD diffractometer using Mo $K\alpha$ radiation (graphite monochromator). The temperature was controlled by an Oxford Cryostream Cooler (700 series, N_2 gas). Data collection, data reduction, and absorption correction were carried out following standard CCD techniques using the software packages Collect and HKL-2000.[48,49] Final cell constants were calculated from 5525 (**1d**) or 8035 (**2b**) reflections from the complete data set. The space groups $P\bar{1}$ (**1d**) and $P\bar{4}n2$ (**2b**) were determined based on systematic absences (or lack thereof) and intensity statistics. The structures were solved by direct methods and refined by full-matrix least-squares minimization and difference Fourier methods (SHELXTL v.6.12).[50,51] All non-hydrogen atoms were refined with anisotropic displacement parameters. All hydrogen atoms were placed in ideal positions and refined as riding atoms with relative isotropic displacement parameters, with the exception of the alkene hydrogen atoms (=C*H*) in **1d**, which were located in the difference Fourier map and refined with a restrained C−H distance (1.00 Å) and relative isotropic displacement parameters (1.2 times the equivalent isotropic value of the bonded carbon atom). For **1d**, the final full-matrix least-squares refinement converged to $R1$ = 0.0264 and $wR2$ = 0.0531 (F^2, all data). The

dx.doi.org/10.1021/ic302570s | Inorg. Chem. 2013, 52, 2564−2580

Scheme 1. Synthesis of *N,N*-Dialkyl-*N′,N″*-diarylguanidines[a]

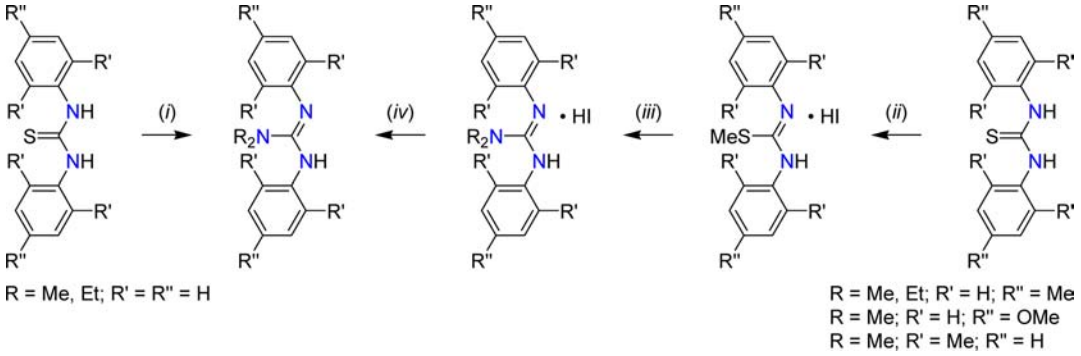

[a](*i*) NHR_2, thf, 0 °C, $N(CH_2Ph)Et_3MnO_4$; (*ii*) MeI, MeOH, reflux, 2 h; (*iii*) NHR_2, MeOH, 70 °C, 7 h; (*iv*) Na_2CO_3, H_2O–Et_2O.

structure of **2b** was inverted during refinement and subsequently refined as an inversion twin, yielding a Flack *x* parameter of 0.08(2). The final full-matrix least-squares refinement converged to *R*1 = 0.0308 and *wR*2 = 0.0873 (F^2, all data). Table 1 and Supporting Information, Table S2 contain crystallographic data and parameters of the data collection and structure refinement. Selected distances and angles are summarized in Supporting Information, Tables S3–S5.

3. RESULTS

3.1. Synthesis and Characterization. In this section, the synthesis and characterization of the *N,N*-dialkyl-*N′,N″*-diarylguanidines, used as ligand precursors for the complexes in this study, and two series of Ir^I complexes of the anionic guanidinates are described (Chart 1). The ligands carry either methyl or ethyl groups on the distal amine nitrogen atom and a range of aryl groups (i.e., Ph, 4-MeC_6H_4, 4-$MeOC_6H_4$, 2,6-$Me_2C_6H_3$, or 2,6-$^iPr_2C_6H_3$) on the coordinating amidinate nitrogen atoms.

3.1.1. N,N-Dialkyl-N′,N″-diarylguanidines. The six neutral guanidines, ArN═C(NR_2)NHAr, were obtained from *N,N′*-diarylthiourea and *N,N*-dialkylamine building blocks (Scheme 1). While the thioureas ArHNC(S)NHAr with Ar = Ph and 4-MeC_6H_4 are commercially available, those with Ar = 4-$MeOC_6H_4$[44] and 2,6-$Me_2C_6H_3$[52] were synthesized by addition of the appropriate aniline, $ArNH_2$, to the corresponding arylisothiocyanate, ArNCS, under conditions reported for the closely related *N,N′*-bis(2,4,6-trimethylphenyl)thiourea.[45] The diphenyl-substituted guanidines PhN═C(NMe_2)NHPh[26] and PhN═C(NEt_2)NHPh[26,53] were prepared in a convenient one-pot procedure by oxidation of *N,N′*-diphenylthiourea with benzyltriethylammonium permanganate in the presence of a 2-fold excess of *N,N*-dialkylamine and were obtained in yields of 70–80% after recrystallization [Scheme 1, step (*i*)]. Other procedures reported for the desulfurization of *N,N′*-diphenylthiourea to produce guanidines involved reaction with $CuSO_4$, SiO_2, and NEt_3 or oxidation with $NaClO_2$ or $NaIO_4$.[54]

For guanidines with substituted aryl groups [i.e., ArN═C(NR_2)NHAr, where R = Me, Ar = 4-MeC_6H_4;[26] R = Et, Ar = 4-MeC_6H_4; R = Me, Ar = 4-$MeOC_6H_4$; and R = Me, Ar = 2,6-$Me_2C_6H_3$[26]], a different method[55] has proven more successful. As shown in Scheme 1, steps (*ii*)–(*iv*), the appropriate thiourea was converted into the *S*-methyl-*N,N′*-diarylisothiourea hydroiodide prior to reaction with an excess of amine to afford the guanidinium iodide. Deprotonation of the latter with Na_2CO_3 gave the guanidine in good overall yield (40–75%, after column chromatography or recrystallization). It should be noted that some of the guanidines in this study are also accessible from diarylcarbodiimides and *N,N*-dimethylamine [i.e., ArN═C(NR_2)NHAr, where R = Me and Ar = Ph, 4-MeC_6H_4 or 4-$MeOC_6H_4$].[56,57] In various other cases, the preparation of tetrasubstituted lithium guanidinates from carbodiimides and lithium amides has been the method of choice.[28h,36,47,58] But, considering the limited availability of carbodiimides, the routes via thioureas appeared to be more straightforward and generally applicable for the targeted range of substitution patterns. The six guanidines described here were characterized by elemental analysis, ^1H and ^{13}C NMR spectroscopy, and EI mass spectrometry (cf. the Experimental Section and ref 26).

3.1.2. (Cyclooctadiene)iridium(I) Complexes. Two different methods were employed for the synthesis of the air-sensitive Ir^I(cod) complexes of the anionic guanidinates, [Ir{ArNC(NR_2)NAr}(cod)], **1a–1g** (Scheme 2). In one method, the

Scheme 2. Synthesis of Alkene Complexes 1a–1g[a]

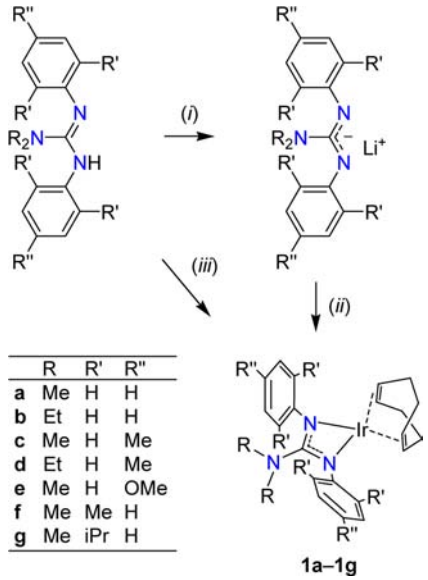

[a](*i*) 1.1 equiv of MeLi, Et_2O, −40 → 20 °C; (*ii*) 0.5 equiv of $[Ir(cod)Cl]_2$, Et_2O; (*iii*) 0.5 equiv of $[Ir(cod)(OMe)]_2$, Et_2O.

guanidine was deprotonated with MeLi at low temperature, followed by reaction of the resulting lithium salt with $[\{Ir(cod)\}_2(\mu\text{-}Cl)_2]$ to yield the yellow Ir^I complex of the guanidinato(1−) ligand. Alternatively, $[\{Ir(cod)\}_2(\mu\text{-}OMe)_2]$ reacted cleanly with the guanidine to give the desired complex, with the bridging methoxido ligands acting as an internal base

dx.doi.org/10.1021/ic302570s | Inorg. Chem. 2013, 52, 2564–2580

for deprotonation of the guanidine. While the deprotonation−transmetalation route allowed the preparation of the diphenyl, bis(4-methylphenyl) and bis(2,6-dimethylphenyl) derivatives **1a**−**1d** and **1f**, it only gave an impure product in poor yield in case of the bis(4-methoxyphenyl) derivative **1e**. This compound was instead directly synthesized from the guanidine using $[\{Ir(cod)\}_2(\mu\text{-}OMe)_2]$. When we tested this method on selected other examples (e.g., **1a** and **1d**), we found it to be more reliable and produce good yields more consistently than the initially used deprotonation−transmetalation method. Complex **1g** (where R = Me and Ar = 2,6-^{i}Pr$_2$C$_6$H$_3$) was prepared from the corresponding lithium guanidinate.[36] The 7 guanidinato complexes are well soluble in nonpolar organic solvents, can be recrystallized from *n*-pentane, and were obtained as analytically pure solids.

All complexes were characterized by ^{1}H and ^{13}C NMR spectroscopy, mass spectrometry, and UV−Vis spectroscopy, and three complexes were also characterized by X-ray crystallography (cf. Section 3.2). Each of the ^{1}H NMR spectra of **1a**−**1f** exhibits only four or five resonance signals attributable to the guanidinato-κ^2N,N' ligand and three to the η^4-cod ligand. Coordination of the guanidinato ligand to the Ir center (**1a**−**1g**) is most clearly discerned from the diagnostic peak of the *N*-methyl or *N*-methylene protons, which undergoes an upfield shift of 0.3−0.6 ppm relative to the neutral guanidine. As expected for an alkene complex, the $\delta(^1H_{C=CH})$ and $\delta(^{13}C_{C=C})$ values for the cod ligands in **1a**−**1g** are significantly lower than those for the free alkene (cf. Section 3.4). While the molecules **1b**, **1d**, and **1f** have nearly C_2 symmetry in the solid state, the NMR spectra indicate fluxional behavior in solution with only one set of resonance signals for the *ortho* (or *ortho* methyl protons in **1f**), *meta* and alkene protons as well as two signals for the cod CH_2 protons. No significant changes were observed in variable-temperature ^{1}H NMR measurements for **1a** and the bulkier **1f** between 20 and −80 °C.

The UV−Vis spectra of the guanidinato complexes exhibit absorption features near 370, 420, and 470 nm (Figure 1).

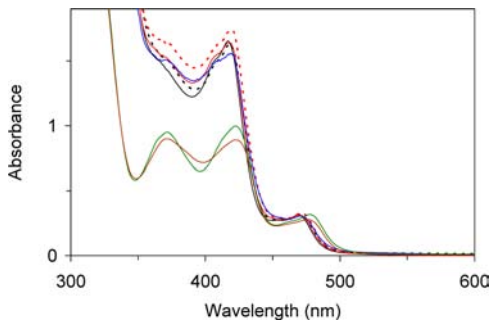

Figure 1. Electronic absorption spectra of 2 mM **1a**−**1g** in toluene (path length, 0.5 cm). Color key: **1a**, solid black line; **1b**, dashed black line; **1c**, solid red line; **1d**, dashed red line; **1e**, solid blue line; **1f**, solid green line; **1g**, solid brown line.

According to the appearance of the bands below 450 nm, the complexes can be divided into two groups. Complexes **1a**−**1e** each display one absorption maximum and a shoulder, whereas the 2,6-dialkylphenyl-substituted complexes **1f** and **1g** show two maxima, each with about half the extinction coefficient observed for **1a**−**1e**.

3.1.3. Dicarbonyliridium(I) Complexes. As shown in Scheme 3, reaction of **1a**−**1g** with an excess of CO produced the dicarbonyls $[Ir\{ArNC(NR_2)NAr\}(CO)_2]$, **2a**−**2g**.

Scheme 3. Synthesis of Dicarbonyl Complexes 2a−2g

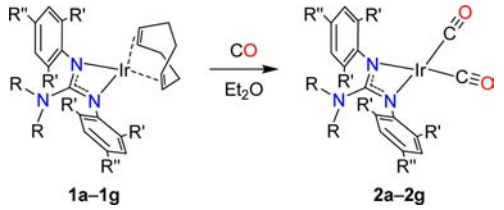

Although the substitution reactions were accompanied by conspicuous color changes (cf. the Experimental Section), the isolated dicarbonyls appear yellow to yellow-orange after recrystallization. The ^{1}H NMR spectra of **2a**−**2g** and the solid-state structure of **2b** (cf. Section 3.2) confirm that the guanidinato(1−) ligands coordinate the Ir center in a symmetric N,N′-chelating binding mode.

Consistent with the presence of two *cis*-coordinated CO ligands, two intense bands were observed in the CO stretching region (ν_{CO}) of the IR spectra of **2a**−**2g**. In *n*-pentane solution, the energies of these bands fall in the ranges of 1980−1983 and 2052−2055 cm^{-1} (*A* and *B* modes), and these data are further discussed in Section 3.4 (Table 3). Bands between 1400 and 1600 cm^{-1}, where CN stretching vibrations of the guanidinato CN_3 core are expected, could be observed in the IR spectra of solid samples. The spectra of the *N*,*N*-dimethyl derivatives **2a**, **2c**, and **2e** (R = Me and Ar = Ph, 4-MeC_6H_4 or 4-MeOC_6H_4) agree strikingly well and each exhibit three principal features at about 1420, 1500, and 1580 cm^{-1} (Supporting Information, Figure S2). Two of the three guanidinato ν_{CN} modes may be expected to fall into this region. For comparison, the CN stretching vibrations of the unsubstituted guanidinium cation were found around 1000 and 1650 cm^{-1} (A_1' and E' modes in D_{3h}).[59] In addition, arene CC stretching (likely at 1500 and 1580 cm^{-1}) and alkyl CH deformation vibrations (<1480 cm^{-1}) may give rise to absorptions in this region. Similarities in the 1400−1600 cm^{-1} region were also observed for the *N*,*N*-diethyl derivatives **2b** and **2d** (R = Et and Ar = Ph or 4-MeC_6H_4) as well as the *N*,*N*′-bis(2,6-dialkylphenyl) derivatives **2f** and **2g** (R = Me and Ar = 2,6-Me$_2C_6H_3$ or 2,6-^{i}Pr$_2C_6H_3$; Supporting Information, Figure S2).

3.2. Crystal Structures. The structures of the cod complexes **1b** and **1f** were briefly reported in a previous publication.[26] Crystallographic analyses were carried out also on single crystals of **1d** and the dicarbonyl complex **2b**. Relevant structural data of these four compounds are summarized in Table 2, and the molecular structures of **1d** and **2b** are shown in Figures 2 and 3.

Complex **1d** crystallized in the triclinic space group $P\bar{1}$. The Ir−N distances are 2.078(2) and 2.087(2) Å, the Ir−C distances are in the range of 2.104(3)−2.115(3) Å, and the N−Ir−N angle is 63.76(9)° (Table 2 and Supporting Information). These parameters are similar to those of **1b** and **1f**, and the Ir−N and Ir−C distances fall into ranges found for Ir^I(cod) complexes of other monoanionic nitrogen-donor ligands.[60−64] The parameters of the guanidinato ligand are consistent with significant lone-pair donation from the NR_2 nitrogen atom into the CN_3 core. In particular, the three C1−N distances of 1.347(4)−1.359(4) Å are essentially equal, indicating effective π-electron delocalization over the three C−N bonds. Also, the bond angle sum for the N3 atom of 359.9(5)° indicates trigonal-planar geometry in agreement with sp^2 hybridization.

dx.doi.org/10.1021/ic302570s | Inorg. Chem. 2013, 52, 2564−2580

Table 2. Selected Structural Data for 1b, 1d, 1f, and 2b[a,b]

	1b	1d	1f	2b
		Interatomic Distances (Å)		
Ir−N1/N2	2.077(2)	2.083(2)	2.087(2)	2.069(6)
Ir−C	2.112(3)	2.109(3)	2.111(3)	1.832(9)
C1−N1/N2	1.355(4)	1.349(4)	1.343(4)	1.359(8)
C1−N3	1.346(4)	1.359(4)	1.354(4)	1.338(11)
C−C (C═C)	1.408(5)	1.418(5)	1.409(5)	
C−O (C≡O)				1.171(11)
		Angles (deg)		
N1−Ir−N2	63.68(9)	63.76(9)	63.72(9)	63.8(3)
N1−C1−N2	108.0(3)	109.3(2)	110.2(2)	107.2(8)
N3−C1−N1/N2	126.1(3)	125.4(3)	124.9(3)	126.4(4)
		Bond Angle Sums (deg)		
∑ (X−N1−X)	349.9(4)	352.4(3)	346.0(3)	354.2(9)
∑ (X−N2−X)	352.4(4)	352.5(3)	352.5(3)	354.2(9)
∑ (X−N3−X)	359.9(5)	359.9(5)	359.8(4)	360.0(9)
		Dihedral Angles (deg)		
N1−C1−N2/N1−Ir−N2	1.3(2)	1.6(3)	3.5(3)	0
C−N3−C/N1−C1−N2[c]	25.6(1)	33.9(2)	18.7(3)	39.6(6)
CN_3/Ar C_6[d]	54.5(1)	48.0(1)	78.6(1)	44.7(3)
	51.7(1)	46.1(1)	74.1(1)	44.7(3)

[a]Numbering scheme for the guanidinate CN_3 atoms as shown for **1d** in Figure 2. Average distances and angles are given for chemically equivalent groups. [b]Data for **1b** and **1f** taken from structures reported in ref 26. [c]Angle between the C−N3−C plane of the NR_2 group and the N1−C1−N2 plane of the $C(NAr)_2$ fragment. [d]Angle between the least-squares planes of the guanidinate CN_3 and aryl ring C atoms.

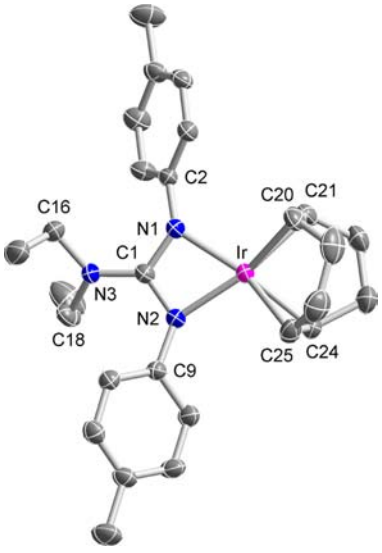

Figure 2. Molecular structure of **1d**, showing the atomic numbering scheme. Displacement ellipsoids are drawn at the 50% probability level; hydrogen atoms have been omitted for clarity. Color key: pink = Ir, blue = N, gray = C.

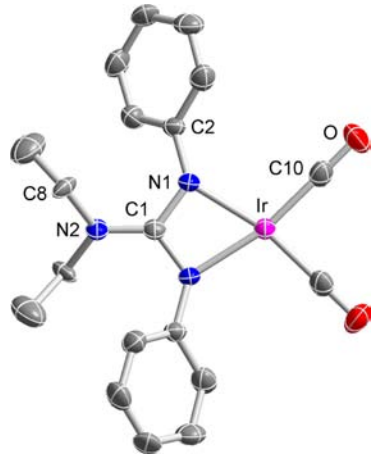

Figure 3. Molecular structure of **2b**, showing the atomic numbering scheme. Displacement ellipsoids are drawn at the 50% probability level; hydrogen atoms have been omitted for clarity. Color key: pink = Ir, blue = N, gray = C, red = O.

Overall, the structural data for the three cod complexes are very similar and do not show any significant electronic influence of the guanidinato substituents (Table 2). Although the difference between the C1−NR_2 (C1−N3) distance and the average C1−NAr (C1−N1/N2) distance seems to vary somewhat for **1b**, **1d**, and **1f**, it is insignificant relative to the uncertainty of the measurement for each complex. The steric influences of the *ortho* methyl substituents in **1f**, however, force the aryl groups into an orientation nearly perpendicular to the guanidinato CN_3 plane [78.6(1) and 74.1(1)°]. Furthermore, a comparison of dihedral angles in the three molecules reveals steric interactions between the NR_2 alkyl and the NAr aryl groups. Thus, the twist angle of the C−N3−C and N1−C1−N2 planes increases with decreasing angles between arene ring and CN_3 planes (Table 2).

The dicarbonyl complex **2b** crystallized in the tetragonal space group $P\bar{4}n2$. The Ir, C1, and N2 atoms are located on a crystallographic C_2 axis (Figure 3). The Ir−N and Ir−C distances are 2.069(6) and 1.832(9) Å, respectively, and the N−Ir−N angle is 63.8(3)° (Table 2 and Supporting Information). The Ir−C and C−O distances are comparable to those of related Ir^I dicarbonyls,[62,65] while almost all parameters involving guanidinato ligand atoms are nearly identical to those of the corresponding cod complex **1b**. The only notable differences are the dihedral angles involving the NR_2 alkyl and NAr aryl groups. The twist angle of the C8−N2−C8#1 and N1−C1−N1#1 planes in **2b** is greater whereas

dx.doi.org/10.1021/ic302570s | Inorg. Chem. 2013, 52, 2564−2580

the angles between arene ring and CN_3 planes are smaller than the corresponding angles in **1b** (Table 2). These differences likely are a consequence of the different sizes of the CO and cod ligands, where the smaller CO ligands in **2b** allow the aryl substituents more rotational freedom.

Inspection of the packing of **2b** revealed short intermolecular contacts between the CO ligands and CH_3 groups of adjacent complexes with O···(H)C9 and C10···(H)C9 distances of 2.357(16) and 2.912(15) Å, respectively. These interactions link four complexes that are related by the 4-fold inversion axis parallel to the *c* axis (Figure 4). Metallophilic interactions,

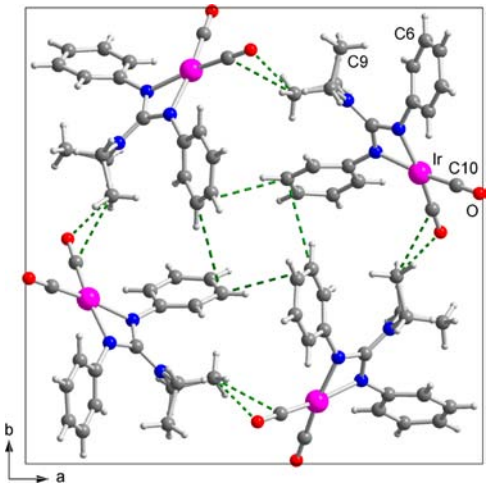

Figure 4. View of the unit cell of **2b** along the crystallographic *c* axis, highlighting intermolecular contacts involving the CO ligands. Color key: pink = Ir, blue = N, gray = C, red = O, light gray = H. Short intermolecular distances (Å): O···(H)C9#2, 2.357(16); C10···(H)-C9#2, 2.912(15); C6···(H)C6#2, 3.756(16). Symmetry operation: #2, 2−*y*, *x*, 2−*z*.

which were observed for some Ir^I dicarbonyls,[66] are not present. In the crystal structures of the cod complexes **1b** and **1d**, close contacts were found between the Ir center and aryl groups of neighboring molecules [for **1b**: Ir···(H)C12, 3.917(4) Å; Ir···(H)C6, 4.021(4) Å; for **1d**: Ir···(H)C11, 3.788(3) Å; Ir···(H)C4, 3.831(3) Å]. Such contacts do not exist in the structure of **1f**; apparently, close approach of an adjacent molecule to Ir is prevented by the methyl groups in ortho positions of the benzene rings (Figure 5).

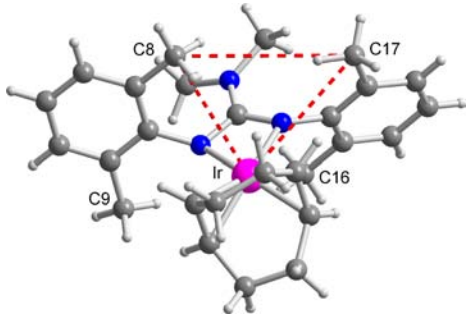

Figure 5. Ball-and-stick representation of **1f** with distances illustrating the steric influences of the *ortho* methyl substituents. Color key: pink = Ir, blue = N, gray = C, light gray = H. Selected distances (Å): Ir···(H)C8, 3.672(3); Ir···(H)C9, 4.316(3); Ir···(H)C16, 4.138(3); Ir···(H)C17, 4.178(4); C8···C17, 4.682(5); C9···C16, 4.943(5).

3.3. Nuclearity in Solution. Both mononuclear[61,62,64,67] and dinuclear[68,69] examples of Ir^I(cod) and $Ir^I(CO)_2$ complexes with bidentate nitrogen-donor ligands are well documented in the literature. (Additional examples can be found in Section 3.4.) Having established the mononuclear solid-state structures of the Ir^I complexes described here, we turned to an examination of the solution nuclearity. The ^1H and ^{13}C NMR spectra of **1a**−**1g** and **2a**−**2g** are consistent with monomeric complexes but do not rule out symmetric or fluxional dimers. For the carbonyls **2a**−**2g**, the observation of two bands in the ν_{CO} region of the solution IR spectra supports a mononuclear structure, whereas three bands may be expected for dinuclear tetracarbonyls.[69] To determine the solution nuclearity of the Ir^I(cod) complexes, we measured the diffusion coefficients (D) of a pair of cod and dicarbonyl complexes, which allowed us to compare their molecular sizes. The diffusion coefficient can be obtained from a stimulated-echo NMR experiment (eq 1, where γ = gyromagnetic ratio, G = gradient strength, δ = length of the gradient pulse, and Δ = delay between the midpoints of the gradients).[43,70] The Stokes−Einstein equation relates D with the hydrodynamic radius (r_H; eq 2, where k = Boltzmann constant, T = absolute temperature, and η = fluid viscosity). Under the assumption of spherical shape, the ratio of the hydrodynamic volumes of two molecules is given by $V_1/V_2 = (D_2/D_1)^3$.[70,71]

$$\ln(I/I_0) = -\gamma^2\delta^2G^2(\Delta - \delta/3)D \quad (1)$$

$$D = kT/6\pi\eta r_H \quad (2)$$

Here, diffusion NMR experiments were carried out on **1a** and **2a** as representative complexes having the same guanidinato ligand. The values of D from measurements in benzene-d_6 are $(8.4 \pm 0.1) \times 10^{-10}$ and $(9.6 \pm 0.2) \times 10^{-10}$ $m^2 \cdot s^{-1}$ for **1a**[38] and **2a**, respectively (cf. the Supporting Information). The ratio of the molecular volumes of **1a** and **2a** in solution is then estimated to be $V_{1a}/V_{2a} = 1.5$. This result agrees reasonably well with the ratio of the crystallographically determined volumes of **1b** and **2b** (Table 1; $V_{1b}/V_{2b} = 1.19$). In contrast, if the cod complex were dinuclear, its molecular size relative to the corresponding dicarbonyl complex would be significantly greater ($2V_{1b}/V_{2b} = 2.39$). Complex **1a** is thus assigned a mononuclear structure in solution. By extension, the heavier members of the cod series are expected to exhibit the same nuclearity, because they were shown by their spectroscopic data to be structurally analogous to **1a**.

To probe whether **1a** and **2a** might convert into dinuclear species at higher concentrations, we recorded NMR and IR spectra at different concentrations. No changes were observed, however, in ^1H NMR spectra of **1a** at concentrations between 5 and 75 mM in $CDCl_3$ and in IR and ^1H NMR spectra of **2a** up to 40 mM in C_6D_6. Thus, the Ir^I(cod) and $Ir^I(CO)_2$ complexes of the smallest guanidinato ligand remain mononuclear at least in these concentration ranges.

3.4. Evaluation of Ligand-Donor Strength. The average CO stretching frequencies of [IrCl(L)$(CO)_2$] complexes have extensively been employed to compare the donor properties of neutral monodentate ligands (L). This parameter has proven particularly useful for ranking a wide range of phosphine[72] and N-heterocyclic carbene[73] ligands, and correlations with related parameters, such as the CO stretching frequencies of corresponding Rh complexes and the Tolman Electronic Parameter, have frequently been made. Studies with alkene complexes, including [IrCl(L)(cod)], [Ir(PPh_3)(L)(cod)]$^+$,

dx.doi.org/10.1021/ic302570s | *Inorg. Chem.* 2013, 52, 2564−2580

and [M(Tp^R)(cod)] complexes [M = Rh, Ir, and Tp = hydrotris(1-pyrazolyl)borate(1−)], have shown that the ^{13}C chemical shifts of the alkene carbon atoms, $\delta(^{13}C_{C=C})$, also reflect the donor strength of other ligands coordinated to the metal center.[12,60,74]

To evaluate the electronic properties of the *N,N*-dialkyl-*N′,N″*-diarylguanidinato(1−) ligands, we utilized both the $\delta(^{13}C_{C=C})$ values of the cod complexes **1a**−**1g** and the average ν_{CO} values of the dicarbonyl complexes **2a**−**2g**. These data are summarized in Table 3. The $\delta(^{13}C_{C=C})$ values of **1a**−**1g** in $CDCl_3$ were found in the range of 58.7−61.0 ppm and the average ν_{CO} values of **2a**−**2g** in *n*-pentane in the range of 2016−2019 cm^{-1}. Both parameters decrease with more electron-donating substituents on the guanidinato ligands (**1a** → **1g**; **2a** → **2g**). These trends reflect increasing π back-donation from Ir into the π^* orbitals of the alkene or CO ligands, which in turn results from increasing electron density at the metal center. Data for **2a** in different solvents clearly show that ν_{CO} is affected by the solvent (Table 3). Even greater variations were observed in the solid state (Supporting Information, Table S1). These may be ascribed to intermolecular interactions, as observed in the crystal structure of **2b** (cf. Section 3.2), or to interactions with the matrix (KBr). Therefore, the solid-state data are not suitable for comparing ligand-donor properties.

Table 3. Alkene ^{13}C Chemical Shifts of 1a−1g and CO Stretching Frequencies of 2a−2g[a]

complex	$\delta(^{13}C_{C=C})$ (ppm)	complex	ν_{CO} (cm^{-1})	avg. ν_{CO} (cm^{-1})
1a	61.0	**2a**	2055, 1983	2019
			2052, 1978[b]	2015[b]
			2051, 1976[c]	2014[c]
			2046, 1970[d]	2008[d]
1b	60.8	**2b**	2055, 1982	2019
1c	60.8	**2c**	2054, 1981	2018
1d	60.7	**2d**	2053, 1980	2017
1e	60.7	**2e**	2053, 1980	2017
1f	58.8	**2f**	2053, 1980	2017
1g	58.7	**2g**	2052, 1980	2016

[a] **1a**−**1g** in $CDCl_3$. **2a**−**2g** in *n*-C_5H_{12}, unless noted otherwise. [b] In Et_2O. [c] In C_6H_6. [d] In Me_2SO.

Literature data for complexes of some monoanionic ligands are compiled in Table 4. Where available, ν_{CO} data for complexes in alkane or chlorinated solvents were selected. Some variation with the solvent may also be expected for the $\delta(^{13}C_{C=C})$ values of the [Ir(L)(cod)] complexes, but the data should provide a reasonable basis for a comparison. Thus, the *N,N*-dialkyl-*N′,N″*-diarylguanidinato ligands are more strongly donating than bis(1-pyrazolyl)borato, β-diketiminato, and 2-(2-pyridyl)pyrrolido ligands. Also included in Table 4 are poly(1-pyrazolyl)borato and tris(2-oxazolinyl)phenylborato ligands as well as the Cp ligand. Where the borato ligands function as κ^2-binding ligands, they are less donating than the guanidinato

Table 4. Alkene ^{13}C Chemical Shifts of [Ir(L)(cod)] Complexes and CO Stretching Frequencies of [Ir(L)(CO)$_2$] Complexes

	[Ir(L)(cod)] complexes		[Ir(L)(CO)$_2$] complexes			
L[a]	solvent	$\delta(^{13}C_{C=C})$ (ppm)	solvent	ν_{CO} (cm^{-1})	avg. ν_{CO} (cm^{-1})	refs
Monoanionic, Bidentate Ligands						
$H_2B(pz)_2$			CH_2Cl_2	2070, 2000	2035	75
$H_2B(pz^{Me2})_2$	CD_2Cl_2	64.1				63
$BDI^{Dipp,CF3}$	C_6D_6	67.6	pentane	2069, 2005	2037	61
$BDI^{Xyl,Me}$	C_6D_6	63.2	pentane	2054, 1986	2020	61
$BDI^{Dipp,Me}$	C_6D_6	62.4	pentane	2053, 1985	2019	61
PyInd	CD_2Cl_2	63.0 (avg.)				76
$PyPyr^{Ph2}$	C_6D_6	63.0 (avg.)	Nujol	2050, 1986	2018	64
$guan^{Ph,Me}$	$CDCl_3$	61.0	pentane	2055, 1983	2019	26[b]
$guan^{Xyl,Me}$	$CDCl_3$	58.8	pentane	2053, 1980	2017	26[b]
$guan^{iPr,iPr}$	$CDCl_3$	58.9				31
$F_2B(I^tBu)_2$			hexane	2052, 1985	2019	65
$H_2B(I^tBu)_2$			hexane	2048, 1979	2014	65
Monoanionic B(pz)$_4$, Tp^R, To^R, and Cp						
$B(pz)_4$-κ^2	CD_2Cl_2	65.1	CH_2Cl_2	2080, 2010	2045	63, 75
Tp^{Me2}-κ^2	$CDCl_3$	63.4				60
Tp^{iPr2}-κ^2	$CDCl_3$	63.6				60
To^P-κ^2/κ^3[c]	C_6D_6	60.8 (avg.)	CH_2Cl_2	2065, 1991	2028	77
To^M-κ^2[c]	thf-d_8	61.3 (avg.)[d]	CH_2Cl_2	2066, 1989	2028	78
To^M-κ^3[c]			CH_2Cl_2	2029, 1934	1982	78
Tp-κ^2[c]			heptane	2074, 2009	2042	79
Tp-κ^3[c]	$CDCl_3$	54.1	heptane	2049, 1974	2012	60, 79
Tp^{Me2}-κ^3			hexane	2039, 1960	2000	80
Cp	$CDCl_3$	45.5	CH_2Cl_2	2033, 1961	1997	81

[a] Ligand acronyms (see ref 82 for a complete list): $H_2B(pz)_2$, dihydrobis(1-pyrazolyl)borate(1−); $BDI^{Ar,Me}$, *N,N′*-diarylpentane-2,4-diiminate(1−); PyInd, 2-(2-pyridyl)indolide(1−); $PyPyr^{Ph2}$, 3,5-diphenyl-2-(2-pyridyl)pyrrolide(1−); $guan^{Ar,R}$, *N,N*-dialkyl-*N′,N″*-diarylguanidinate(1−); $H_2B(I^tBu)_2$, bis(3-*tert*-butylimidazolin-1-yl-2-ylidene)dihydroborate(1−); Tp, hydrotris(1-pyrazolyl)borate(1−); To, tris(2-oxazolinyl)phenylborate(1−). [b] This work. [c] Solutions of [Ir(To^P)(cod)], [Ir(To^M)(CO)$_2$], and [Ir(Tp)(CO)$_2$] were reported to contain mixtures of complexes with κ^2- and κ^3-binding ligands. [d] Data for [Ir(To^M)(cod)]·LiCl.

dx.doi.org/10.1021/ic302570s | *Inorg. Chem.* 2013, 52, 2564−2580

ligands in this study, whereas κ^3-binding borates are more donating.

Not included in the table but briefly compared in the following are several more elaborate hybrid ligands that also possess a monoanionic nitrogen-donor set. For example, bis(pyridyl)dihydroisoindolido-κ^2 ligands [avg. $\delta(^{13}C_{C=C})$ = 65.1 and 65.4 ppm],[83] one pyridine−amine−pyrrolido-κ^2 ligand [avg. $\delta(^{13}C_{C=C})$ = 61.9 ppm],[84] and one imine−indolido ligand [avg. $\delta(^{13}C_{C=C})$ = 61.2 ppm][62] appear less electron-releasing in their [Ir(L)(cod)] complexes than the guanidinato ligands, while pyridazine−amido ligands seem to cover a wider range of donor properties [avg. $\delta(^{13}C_{C=C})$ = 56.2−66.8 ppm].[85] Lastly, cationic carbonyl and cod complexes of neutral, bidentate nitrogen-donor ligands, such as phenanthroline derivatives [ν_{CO} (MeCN) = 2055−2059 cm^{-1}][86] and bis(1-pyrazolyl)methane and bis(2-imidazolyl)methane derivatives [$\delta(^{13}C_{C=C})$ = 66.7−70.3 ppm],[87] exhibit greater ν_{CO} and $\delta(^{13}C_{C=C})$ values. These data may be a consequence not only of weaker donor strength but also of the positive charge of the complex.[88]

3.5. Reaction of (Alkene)iridium(I) Complexes with O_2 and Characterization of (Alkene)peroxoiridium(III) Intermediates. The solution reactivity of the Ir^I(cod) complexes with different guanidinato substituents toward O_2 was investigated by UV−Vis spectroscopy. The absorption bands shown in Figure 1 decayed, giving spectra that are featureless above 400 nm, before a broad absorption increase was observed in a subsequent slower phase. Concomitant with these spectral changes, the color of the solutions turned from bright yellow to pale yellow to dark green. The intermediate in the reaction of **1a** with O_2 was recently characterized as the mononuclear (alkene)peroxo complex [Ir{PhNC(NMe$_2$)NPh}(cod)(O_2)], **3a**, on the basis of one- and two-dimensional NMR techniques and IR spectroscopy (Scheme 4).[38]

Scheme 4. Generation of (Alkene)peroxo Intermediates 3a−3e

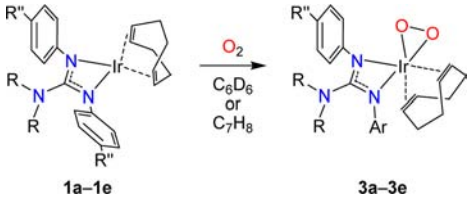

Time courses of the O_2 reactions of **1a−1f** in toluene at 0 °C to form the corresponding intermediates **3a−3f** are shown in Figure 6. Under these conditions, the half-lives range from about 10 min to 1 h [$t_{1/2} \approx$ 1300 s (**1a**), 1100 s (**1b**), 1100 s (**1c**),[46] 850 s (**1d**), 700 s (**1e**), and 1 h (**1f**)]. The data are consistent with expected electronic and steric substituent effects. Specifically, the half-lives decrease with more electron-donating substituents in the para position of the benzene rings (**1a** > **1c** > **1e**) and in the NR_2 group (**1a** > **1b**; **1c** > **1d**) due to increasing destabilization of the Ir^I oxidation state (or stabilization of the Ir^{III} state). Interestingly, substitution in either one of the two ligand positions brings about the same rate-accelerating effect (**1b** ≈ **1c**), which may reflect the conjugated nature of the guanidinato core. On the other hand, substituents in the ortho positions of the benzene rings have a decelerating effect (**1f**). This effect is likely due to steric hindrance, as an increased level of steric protection of the Ir center in **1f** is evident from a comparison of the crystallographically determined structures of **1b**, **1d**, and **1f** (Figures 2 and 5 and ref 26).

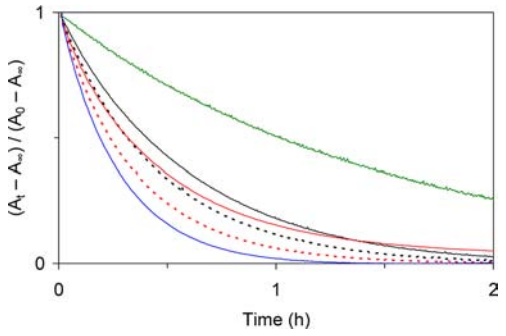

Figure 6. Time courses of the reactions of 2 mM **1a−1f** in toluene with O_2 at 0 °C as monitored by electronic absorption spectroscopy (path length, 0.5 cm). Color key: **1a**, solid black line (λ = 417 nm); **1b**, dashed black line (λ = 418 nm); **1c**, solid red line (λ = 418 nm); **1d**, dashed red line (λ = 419 nm); **1e**, solid blue line (λ = 419 nm); **1f**, solid green line (λ = 423 nm).

More dramatic differences were discovered at higher temperature. In contrast to **1a−1e**, **1f** decayed only partially when treated with O_2 at 20 °C, suggesting that the reaction is reversible and that O_2 binding is favored at lower temperature. Further investigation revealed that **1f** can be regenerated upon removal of O_2. First, reaction of **1f** in toluene with O_2 at 20 °C resulted in only about 70% of the absorbance change expected for complete decay (Figure 7). When the solution was

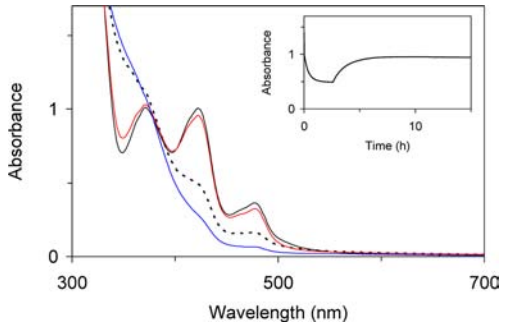

Figure 7. Electronic absorption spectra of 2 mM **1f** in toluene at 20 °C (solid black line), the solution at maximum decay of **1f** in the reaction with O_2 (dashed black line; t = 2.5 h), and **1f** regenerated upon removal of O_2 (solid red line; t = 10 h; path length, 0.5 cm). The spectrum showing full decay of **1f** was obtained from the reaction of 2 mM **1f** in toluene with O_2 at 0 °C after 7.5 h (solid blue line). Inset: Time course of the reaction of **1f** in toluene with O_2 at 20 °C and regeneration of **1f** after removal of O_2 (λ = 423 nm).

subsequently purged with Ar to remove O_2, the absorption bands of **1f** began to regain intensity and were eventually fully recovered. Thus, binding of O_2 to **1f** is fully reversible at 20 °C (Scheme 5). An analogous experiment with **1a** showed no significant reformation. Instead, intermediate **3a**, formed from reaction of **1a** with O_2, decayed under Ar in nearly the same way as under O_2, with a weak shoulder at 420 nm indicating the presence of a minimal amount of **1a** (Supporting Information, Figure S4). Complex **1g** with bulkier diisopropyl substituents reacted with O_2 even more slowly than **1f**, and only partial decay was observed even at −25 °C. It thus appears that the equilibrium between the Ir^I(cod) complex and its O_2 adduct is shifted further to the left for **1g** than for **1f**.

dx.doi.org/10.1021/ic302570s | Inorg. Chem. 2013, 52, 2564−2580

Scheme 5. Reversible Formation of (Alkene)peroxo Intermediates 3f and 3g

For characterization purposes, the intermediates were generated at a higher concentration. When **3a** was generated from 20 mM **1a** in benzene-d_6 at 20 °C, it accumulated in a yield of 75%. The corresponding intermediates in the reactions of **1b**−**1e** with O_2 also can be generated in high yield (Scheme 4). Under similar conditions, **3b**−**3e** accumulated in about 2−3 h and decayed within 20 h of initiation of the reaction. The shortest formation time and longest decay time were observed for **3e**, showing that electron-donating substituents prolong the lifetime of the (alkene)peroxo intermediate. Like for **3a**, the ^{1}H NMR spectra of **3b**−**3e** indicate desymmetrization, compared to their respective Ir^I precursors, and the presence of unmodified guanidinato and cod ligands (cf. the Experimental Section). Specifically, each of the spectra exhibits two sets of resonance signals attributable to two inequivalent guanidinato aryl groups, four distinct cod alkene signals [$\delta(^1H)$ = 4.0−4.8 ppm], and several multiplets accounting for four CH_2 groups. Only one singlet is observed for the *N*-methyl protons in **3a**, **3c**, and **3e**, suggesting that rotation about the guanidinato C−NMe_2 bond is facile. Similarly, two signals are found for the diastereotopic NCH_2 protons in **3b** and **3d**. Overall, the ^{1}H NMR data of **3a**−**3e** show that these intermediates adopt very similar structures.

Coordination of the peroxo ligand to Ir was confirmed by IR spectroscopy on solid samples. The samples were prepared by solvent removal, and the integrity of the intermediates was verified by ^{1}H NMR spectroscopy on redissolved samples. Attempts to grow single crystals of the intermediates have been hampered by their limited lifetime in solution. For each intermediate, one medium strong band was observed in the OO stretching region (ν_{OO}) near 860 cm^{-1} (Table 5 and Supporting Information, Figures S5−S9). In addition, two weak bands that can be assigned to IrO stretching modes (ν_{IrO}) were located at about 575 and 460 cm^{-1}. These three bands were not observed in the spectra of the decay products of **3b**−**3e** (Supporting Information, Figures S5−S9). For **3a**, the assignments were previously corroborated by an ^{18}O-isotope-labeling study, with good agreement between observed and calculated isotope shifts (Table 5). The energies of ν_{OO} in **3a**−**3e** fall into the range of 800−900 cm^{-1} determined for other (η^2-peroxo)iridium(III) complexes, which include complexes with phosphine,[18,19,21b,89,90] PCP pincer,[91] N-heterocyclic carbene,[92] dithiocarbamato,[93] and diimine[94] ligands. For example, values of 855−858 cm^{-1} were reported for the "O_2 adduct" of Vaska's complex, $[IrCl(PPh_3)_2(CO)(O_2)]$,[19,21b,89] while energies of 880 and 850 cm^{-1} were found for the (alkene)peroxo complexes $[IrCl(PPh_3)_2(C_2H_4)(O_2)]$ and [Ir(phen)(cod)$(O_2)]^+$, respectively.[21,22] Data for ν_{IrO} have only occasionally been mentioned in the literature (ca. 500−650 cm^{-1}).[94,95] Comparison of the ν_{OO} data of **3a**−**3e** shows that the band shifts to lower energies in the order **3a**, **3b** > **3c**, **3d** > **3e**. Given the similar structures of these intermediates (vide supra), this trend may reflect increasing population of peroxide π^* orbitals (i.e., a more reduced peroxo ligand) with more electron-donating guanidinato ligands.

Table 5. OO and IrO Stretching Frequencies of 3a−3f[a]

complex	ν_{OO} (cm^{-1})	ν_{IrO} (cm^{-1})
3a[b]	865	575, 459
3a-$^{18}O_2$[b]	813	550, 442
calcd[b]	816	545, 435
3b	865	576, 459
3c	862	575, 459
3d	862	575, 458
3e	857	573, 457
3f	872	572, 459

[a]Solid state (KBr disk). [b]From ref 38.

We also attempted to generate the (alkene)peroxo intermediate of the bis(2,6-dimethylphenyl)-substituted ligand, **3f**, at a higher concentration that is more suitable for characterization (15−20 mM **1f**). Because of the reversibility of this reaction, the maximum accumulation of **3f** was lower than for the other intermediates (ca. 60% after about half a day), and **1f** was still present at that time (Supporting Information, Figure S11). Both **1f** and **3f** eventually decayed over the course of 2 weeks. Relevant IR data of **3f** are included in Table 5 (Supporting Information, Figure S10). At first glance, the high value of 872 cm^{-1} for ν_{OO} may seem surprising, because based on ligand-donor strength and the trend observed for **3a**−**3e** one might expect a lower value for **3f**. Instead, the higher wavenumber may be a consequence of steric pressure exerted by the *ortho* methyl substituents on the peroxo ligand in **3f**, which may cause structural changes and perhaps weakens Ir−peroxo binding (i.e., a less reduced peroxo ligand). The ^{1}H NMR data of **3f** are consistent with greater steric constraints, showing a wider shift range for the cod alkene resonance signals (compared to **3a**−**3e**) and four distinct singlets for the ortho methyl groups (cf. the Experimental Section).

3.6. Reactivity of (Alkene)peroxoiridium(III) Intermediates. To gain insight into the reactivity of the (alkene)peroxoiridium(III) intermediates, we investigated reactions with PPh_3 and CO as well as their self-decay leading to cod oxygenation.

Peroxo complexes of late transition metals frequently oxidize phosphines to phosphine oxides.[18,91,96] In agreement with this pattern, intermediate **3a** reacted in deoxygenated solution with PPh_3 to yield $OPPh_3$.[38] The same intermediate also reacted with CO, producing a carbonato complex, **4a**, as well as the dicarbonyl complex **2a** and free cod (eq 3). The carbonato complex was identified by ESI mass spectrometry and IR spectroscopy and is tentatively assigned as [Ir{PhNC(NMe_2)NPh}(cod)(CO_3)]. The masses and isotope distribution patterns of peaks at m/z = 600 and 622 match the formulations {**4a** + H}$^+$ and {**4a** + Na}$^+$, respectively, while the presence of a chelating carbonato-κ^2O,O' ligand[97−99] was inferred from a band in the solid-state IR spectrum at 1690 cm^{-1} (ν_{CO}).[100] These assignments were confirmed by an ^{18}O-labeling experiment using **3a**-$^{18}O_2$ and CO (m/z = 604 and 626). The appearance of a new IR absorption at 1667 cm^{-1} indicated some scrambling of the labeled oxygen atoms into the terminal position of the carbonato ligand.[99] Also identified in the IR spectra was complex **2a** by its characteristic absorption bands in the 1900−2100 cm^{-1} region. Both **2a** and free cod could be

dx.doi.org/10.1021/ic302570s | Inorg. Chem. 2013, 52, 2564−2580

quantified by ^{1}H NMR spectroscopy, and the yields were about 30% for **2a** and 40% for cod (with respect to Ir).

$$[Ir^{III}(L)(cod)(O_2)] + \text{excess CO} \rightarrow [Ir^{III}(L)(cod)(CO_3)] + [Ir^{I}(L)(CO)_2] + \text{cod} \quad (3)$$

Formation of carbonato complexes from reaction of peroxo complexes with CO has been described.[98,99] It is conceivable that the carbonato complex **4a** formed here reacts further by substitution of CO for the cod ligand and reduction to afford **2a**. Another possible pathway to **2a** involves reaction of CO with the Ir^{I}(cod) complex **1a**, because a small amount of this complex could be regenerated from **3a** when O_2 is absent (Section 3.5) and conversion of **1a** into **2a** is facile (Section 3.1.3). In either case, the formation of **2a** differs somewhat from the quantitative displacement of O_2 from a Rh(O_2^{2-}) complex by a stoichiometric amount of CO.[101] Irrespective of the mechanism, the production of nearly equimolar amounts of **2a** and free cod confirms the presence of the Ir(L)(cod) entity in intermediate **3a**.

In the absence of added substrates, intermediates **3a**–**3f** decayed to dark green products. In principle, self-decay of the (alkene)peroxo intermediates may be initiated in several different ways, including oxidation of the guanidinato or alkene ligands or dissociation of superoxide. Attack by the peroxo ligand may be more facile at the alkene (cod) than at the guanidinato aryl or alkyl groups. Unfortunately, the identity of the decay products was not accessible from NMR spectroscopy, because the spectra exhibit unresolved, broad resonances in the ranges of 6.5–7.5 and 1–3 ppm. Yet, we were able to extract the guanidinato ligand from the decay products of **3a** and recover it in a substantial yield, demonstrating that it remained largely intact throughout the decay of the (alkene)peroxo intermediate (cf. the Experimental Section). Furthermore, the decay under N_2 of intermediates without ortho substituents gave similar results as under O_2, with the only difference being the presence of a small amount of **1** (e.g., 10–15% of **1a**, **1d**, or **1e**), which is consistent with a minor degree of reversibility in the formation of **3a** (cf. Section 3.5).

The ESI mass spectra of the decay products of **3a**–**3f** indicate that oxygen was retained upon decay. The assignments of the peaks listed in Table 6 to {**3** − OH}$^+$ and {**3** − H}$^+$ are supported by their isotope distribution patterns, the mass shifts observed for complexes with different guanidinato ligands, and an ^{18}O-labeling experiment for **3a**. The monooxygenated products are consistent with (oxo-η^2-cyclooctenyl) complexes, [Ir(L)(η^2-C_8H_{11}O-κC)(OH)], upon dissociation of hydroxide ion. Mechanisms for alkene oxygenation via (alkene)peroxo intermediates usually invoke conversion into 3-metalla-1,2-dioxolanes, if the reaction takes place at a single metal center.[7,10] Examples of 3-rhoda- and 3-irida-1,2-dioxolanes have been reported,[16,17,20] and rearrangement into β-oxoalkyl complexes has been described in several cases.[17,102] On the basis of these precedents, we propose that formation of an (oxo-η^2-cyclooctenyl) complex (**B**) proceeds from **3** by alkene insertion into the Ir–O bond to afford an iridadioxolane, [Ir(L)(η^2-$C_8H_{12}O_2$-$\kappa C,\kappa O$)] (**A**), which in turn undergoes O–O bond cleavage and hydrogen migration (Scheme 6). The

Table 6. Mass-to-Charge Ratios (m/z) from the ESI Mass Spectra of the Decay Products of 3a–3g[a]

complex	{LH + H}$^+$	{M − O_2H}$^+$	{M − OH}$^+$	{M − H}$^+$
3a[b]	240.2	538.3	554.2	570.1
calcd	240.2	538.2	554.2	570.2
3a-$^{18}O_2$[b]	240.2	538.4	556.3	574.3
3b	268.1	566.2	582.1	598.1
3c	268.1	566.2	582.1	598.1
3d	296.2	594.2	610.1	626.1
3e	300.2	598.3	614.2	630.1
3f	296.2	594.3	610.2	
3g	408.4	706.5	722.3	

[a]LH = ArN=C(NR$_2$)NHAr; M = **3a**–**3g**. [b]From ref 38.

Scheme 6. Proposed Mechanism for the Decay of 3[a]

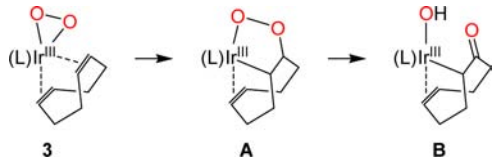

[a]L = {ArNC(NR$_2$)NAr}$^-$.

dioxygenated species observed in the mass spectra may be related to the iridadioxolanes. Also observed were products that do not contain oxygen, that is, {**3** − O_2H}$^+$ (Table 6), and are consistent with (η^5-cycloocta-2,5-dien-1-yl) complexes, [Ir(L)(η^5-C_8H_{11})]$^+$ (**C**). These products might hint at the existence of an unproductive decay channel by dissociation of $O_2^{\bullet-}$ from **3** to give Ir^{II}(cod) complexes (eq 4).[103] Such species tend to undergo allylic hydrogen atom transfer that affords Ir^{III}(η^2-ene-η^3-enyl) species (**C**),[104] as indicated in eq 5.

$$[Ir^{III}(L)(\eta^4\text{-}C_8H_{12})(\eta^2\text{-}O_2)] \rightarrow [Ir^{II}(L)(\eta^4\text{-}C_8H_{12})]^+ + O_2^{\bullet-} \quad (4)$$

$$2[Ir^{II}(L)(\eta^4\text{-}C_8H_{12})]^+ \rightarrow [Ir^{III}(L)(\eta^5\text{-}C_8H_{11})]^+ + [Ir^{III}(L)(\eta^4\text{-}C_8H_{12})H]^+ \quad (5)$$

Taken together, these results suggest that the decay of intermediates **3a**–**3f**, at least in part, led to oxygenation of the cod ligand. In addition to the presence of multiple products (**A**–**C**), it is likely that geometrical isomers of **A** and **B** and possibly hydroxo- or oxo-bridged dimers of **B** were formed, and a mixture of several such products might have led to the convoluted NMR data. The integrity of the guanidinato ligand, however, was established by its recovery from the product mixture.

We therefore sought for ways to extrude the oxygenated cod fragment from the decay products of **3**. While heating of the solution did not cause any changes (1 d at 70 °C), reaction with cod under the same conditions afforded 4-cycloocten-1-one and **1** (Scheme 7). For example, the yields from the reaction of the decay products of **3a** with 2 equiv of cod were 90 and 30%

Scheme 7. Oxygenation of 1,5-Cyclooctadiene from 3a–3f[a]

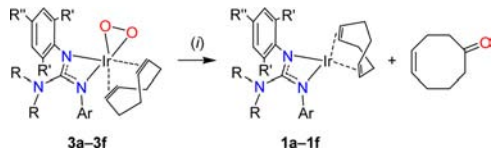

[a](*i*) 1. C_6D_6, 20 °C, 1 d; 2. Two equiv of cod, C_6D_6, 70 °C, 1 d.

dx.doi.org/10.1021/ic302570s | Inorg. Chem. 2013, 52, 2564–2580

(based on Ir) for 4-cycloocten-1-one and **1a**, respectively.[38] Similar results were obtained for reactions employing the decay products of **3b**−**3e** with yields of 75−90% for 4-cycloocten-1-one and 25−35% for **1**. Electron-donating substituents on the guanidinato ligand thus do not exhibit an appreciable effect in this reaction. In contrast, with the sterically more demanding bis(2,6-dimethylphenyl)-substituted guanidinato ligand, the yields were roughly halved (45 and 13%). Overall, the significantly different yields of 4-cycloocten-1-one and **1** common to all of the cod reactions suggest that these products are formed in two different steps. A mechanism accounting for both products could involve cod C−H bond activation by the (oxo-η^2-cyclooctenyl) complex (**B**) to give 4-cycloocten-1-one and an (η^5-cycloocta-2,5-dien-1-yl) complex, [Ir(L)(η^5-C_8H_{11})(OH)], followed by reaction with a second equivalent of cod by alkene insertion into the Ir−OH bond[105] and β-hydrogen migration to yield 4-cycloocten-1-one and an (η^5-cycloocta-2,5-dien-1-yl)hydrido complex, [Ir(L)(η^5-C_8H_{11})H], which then could regenerate **1**.

4. DISCUSSION

We have synthesized [Ir(L)(cod)] and [Ir(L)$(CO)_2$] complexes supported by seven different *N*,*N*-dialkyl-*N*′,*N*″-diarylguanidinato ligands and investigated the formation of [Ir(L)(cod)(O_2)] intermediates, along with the ensuing alkene oxygenation.

Ligand-Donor Strength. The electron-donating ability of the guanidinato ligands was evaluated using the CO stretching frequencies of the dicarbonyl complexes and the alkene ^{13}C chemical shifts of the cod complexes. Based on these parameters and a comparison with literature data for complexes of other monoanionic ligands, the donor strength of these ligands increases in the order $B(pz)_4$-κ^2 < Tp^{R2}-κ^2 < $BDI^{Ar,Me}$ ≈ $PyPyr^{Ph2}$ < $guan^{Ar,R}$ < Tp^{R2}-κ^3 < Cp. This ranking is in good agreement with results from a recent study using [Rh(L)$(CO)_2$] complexes to compare the $PyPyr^{R2}$ system with various other monoanionic ligands.[106] In that study, the ν_{CO} values given for complexes of relevant nitrogen donors decrease in the order Tp^{R2}-κ^2 > $PyPyr^{R2}$ ≈ $BDI^{Ar,R}$ > $PyPyr^{tBu2}$ > $amidinate^{Cy,Fc}$ (where R = CF_3). Data for guanidinato ligands are not available, but they usually function as stronger donors than amidinato ligands.[27]

Reversible and Irreversible Formation of (Alkene)peroxoiridium(III) Intermediates. The trends observed for the reactivity of **1a**−**1g** toward O_2 conform with electronic and steric factors (Section 3.5). The ligand substituents also affect the reversibility of the O_2 reaction of **1**. For complexes without ortho substituents (**1a**−**1e**), the reaction is virtually irreversible and allows the generation of **3a**−**3e** in high yield. In contrast, O_2 binding is reversible for the bis(2,6-dialkylphenyl) derivatives **1f** and **1g**. From the structures of the Ir^I complexes and the spectroscopic differences between **3f** and **3a**−**3e**, it is clear that the ortho substituents create steric pressure that likely weakens O_2 binding to Ir. Others have shown that O_2 binding can be tuned by differences in ligand polarizability.[107] Steric effects on O_2 reactivity at Ir have been described in early work by Vaska, but there ortho methyl substituents on the triarylphosphine ligands block the reactivity entirely.[108]

Alkene Oxygenation. Notably, the new intermediates **3a**−**3f** decayed to oxygenate the alkene ligand. (Oxo-η^2-cyclooctenyl) complexes were identified from the decay products, and subsequent reaction with added cod afforded significant yields of 4-cycloocten-1-one and **1a**−**1f**. These results are remarkable in light of the limited reactivity of known (alkene)peroxo complexes. C−O bond formation has only been reported for [$IrCl(PPh_3)_2(C_2H_4)(O_2)$].[25] Because of PPh_3 co-oxidation, the mechanism of this reaction must necessarily differ from that of cod oxygenation in **3a**−**3f**. On the other hand, the Rh^{III}(alkene)(O_2^{2-}) complex even reverted back to its Rh^I(alkene) precursor under O_2 loss when heated above 60 °C.[23] The lack of reactivity between the alkene and peroxo ligands was ascribed to their unique relative disposition at the metal center. In all three crystal structures, the O_2^{2-} ligand and the C═C group are nearly coplanar and bound to the metal center in a butterfly fashion.[23,24] It was speculated that this geometry may be unfavorable for C−O bond formation.[10,23] In contrast, at least one of the two C═C groups in **3a**−**3f** must be positioned out of plane relative to the O_2^{2-} ligand (while the other one may be in plane with the O_2^{2-} ligand). It would thus appear that such an orthogonal arrangement is more favorable for an interaction between these ligands that can lead to C−O bond formation. Stereochemical factors may then indeed be critical for alkene oxygenation at Rh and Ir.

An (oxo-η^2-cyclooctenyl) complex of Ir was previously reported, but that was obtained by oxidation of an Ir^I(cod) complex with H_2O_2 (in the presence of acid), which necessarily involves a different mechanism.[109] Similar 2-oxoethyl complexes of both Rh and Ir were obtained from reactions of $M^I(C_2H_4)$ complexes in the solid state with gaseous O_2 via 3-metalla-1,2-dioxolanes.[17,102] It is possible that the formation of the 3-metalla-1,2-dioxolanes proceeded through (alkene)peroxo intermediates akin to those described here, although radical pathways[9,110] have also been considered. Cleavage of the oxygenated organic fragment from the metal by heating or protonation has not been achieved for any of these species. More successful has been the elimination of organic products from 2-metallaoxetanes,[15] which have been obtained by oxidation of M^I(alkene) complexes with H_2O_2 (M = Rh, Ir),[9] by reaction of $M_2(\mu$-$O)_2$ complexes with alkenes (M = Pt, Au),[111] or from Pt(alkene)(OH) complexes.[5,112] In a rare case of a 2-rhodaoxetane prepared using O_2, 4-cycloocten-1-one could be eliminated by reaction with PMe_3 or CO.[113] The O_2 activation step in the generation of the 2-rhodaoxetane[14] was proposed to involve an (alkene)peroxo species similar to **3**, before intermolecular trapping eventually leads to C−O bond formation.

5. CONCLUSION

The modular synthesis of the *N*,*N*-dialkyl-*N*′,*N*″-diarylguanidine ligand precursors enabled us to produce a series of [Ir{ArNC(NR_2)NAr}(cod)] complexes (**1a**−**1g**) for a systematic investigation of their reactivity. Activation of O_2 by these complexes proceeds with high selectivity yielding the corresponding (alkene)peroxoiridium(III) intermediates (**3a**−**3e**). Intriguingly, the introduction of sterically encumbering substituents (**1f** and **1g**) causes a marked switch from irreversible to reversible formation. In addition to the spectroscopic characterization of **3a**−**3f**, each group in intermediate **3a** was probed by its chemical behavior. In particular, the peroxo ligand oxygenated PPh_3 to $OPPh_3$, the Ir(L)(cod) entity could be converted by reaction with CO into [Ir(L)$(CO)_2$] and free cod, and the free guanidine was recovered from the decay products of **3a**. The new intermediates are quite unique, because only a small number of (alkene)peroxo complexes has been described in the

dx.doi.org/10.1021/ic302570s | Inorg. Chem. 2013, 52, 2564−2580

literature. Moreover, the C−O bond formation chemistry observed for **3a**−**3f**, along with regeneration of the respective Ir^{I}(cod) complexes **1a**−**1f**, demonstrates that (alkene)peroxo species could be relevant to catalytic alkene oxygenation with O_2.

■ ASSOCIATED CONTENT

Supporting Information

Additional spectroscopic data for **2a**−**2g** and **3a**−**3f** (Figures S1−S11 and Tables S1 and S6, PDF), details of the crystal structure determinations (Tables S2−S5, PDF), and crystallographic information files of **1d** and **2b** (CIF). This material is available free of charge via the Internet at http://pubs.acs.org.

■ AUTHOR INFORMATION

Corresponding Author

*E-mail: jan-uwe-rohde@uiowa.edu.

Notes

The authors declare no competing financial interest.

■ ACKNOWLEDGMENTS

This research was supported by the American Chemical Society Petroleum Research Fund (46587-G3) and the National Science Foundation (CAREER Award CHE-1057163). We thank Dr. Dale C. Swenson for the collection of X-ray diffraction data.

■ REFERENCES

(1) Hill, C. L.; Weinstock, I. A. *Nature* **1997**, *388*, 332.
(2) (a) van Santen, R. A.; Kuipers, H. P. C. E. *Adv. Catal.* **1987**, *35*, 265. (b) Serafin, J. G.; Liu, A. C.; Seyedmonir, S. R. *J. Mol. Catal. A: Chem.* **1998**, *131*, 157. (c) Monnier, J. R. *Appl. Catal., A* **2001**, *221*, 73. (d) Barteau, M. A. *Top. Catal.* **2003**, *22*, 3.
(3) (a) Stahl, S. S. *Angew. Chem., Int. Ed.* **2004**, *43*, 3400. (b) Cornell, C. N.; Sigman, M. S. *Inorg. Chem.* **2007**, *46*, 1903. (c) Muzart, J. *Tetrahedron* **2007**, *63*, 7505. (d) Keith, J. A.; Henry, P. M. *Angew. Chem., Int. Ed.* **2009**, *48*, 9038.
(4) Punniyamurthy, T.; Velusamy, S.; Iqbal, J. *Chem. Rev.* **2005**, *105*, 2329.
(5) Vedernikov, A. N. *Acc. Chem. Res.* **2012**, *45*, 803.
(6) (a) Boisvert, L.; Goldberg, K. I. *Acc. Chem. Res.* **2012**, *45*, 899. (b) Konnick, M. M.; Stahl, S. S. *J. Am. Chem. Soc.* **2008**, *130*, 5753. (c) Konnick, M. M.; Decharin, N.; Popp, B. V.; Stahl, S. S. *Chem. Sci.* **2011**, *2*, 326. (d) Szajna-Fuller, E.; Bakac, A. *Inorg. Chem.* **2010**, *49*, 781.
(7) (a) Mimoun, H.; Perez Machirant, M. M.; Seree de Roch, I. *J. Am. Chem. Soc.* **1978**, *100*, 5437. (b) Mimoun, H. *Pure Appl. Chem.* **1981**, *53*, 2389. (c) Read, G. *J. Mol. Catal.* **1988**, *44*, 15.
(8) (a) Drago, R. S.; Zuzich, A.; Nyberg, E. D. *J. Am. Chem. Soc.* **1985**, *107*, 2898. (b) Faraj, M.; Martin, J.; Martin, C.; Bregeault, J.-M.; Mercier, J. *J. Mol. Catal.* **1985**, *31*, 57. (c) Atlay, M. T.; Preece, M.; Strukul, G.; James, B. R. *J. Chem. Soc., Chem. Commun.* **1982**, 406.
(9) de Bruin, B.; Budzelaar, P. H. M.; Gal, A. W. *Angew. Chem., Int. Ed.* **2004**, *43*, 4142.
(10) Tejel, C.; Ciriano, M. A. *Top. Organomet. Chem.* **2007**, *22*, 97.
(11) Day, V. W.; Klemperer, W. G.; Lockledge, S. P.; Main, D. J. *J. Am. Chem. Soc.* **1990**, *112*, 2031.
(12) de Bruin, B.; Brands, J. A.; Donners, J. J. J. M.; Donners, M. P. J.; de Gelder, R.; Smits, J. M. M.; Gal, A. W.; Spek, A. L. *Chem.—Eur. J.* **1999**, *5*, 2921.
(13) Flood, T. C.; Iimura, M.; Perotti, J. M.; Rheingold, A. L.; Concolino, T. E. *Chem. Commun.* **2000**, 1681.
(14) Tejel, C.; Ciriano, M. A.; Sola, E.; del Rio, M. P.; Rios-Moreno, G.; Lahoz, F. J.; Oro, L. A. *Angew. Chem., Int. Ed.* **2005**, *44*, 3267.
(15) Dauth, A.; Love, J. A. *Chem. Rev.* **2011**, *111*, 2010.
(16) Krom, M.; Coumans, R. G. E.; Smits, J. M. M.; Gal, A. W. *Angew. Chem., Int. Ed.* **2001**, *40*, 2106.
(17) Krom, M.; Peters, T. P. J.; Coumans, R. G. E.; Sciarone, T. J. J.; Hoogboom, J.; ter Beek, S. I.; Schlebos, P. P. J.; Smits, J. M. M.; deGelder, R.; Gal, A. W. *Eur. J. Inorg. Chem.* **2003**, 1072.
(18) (a) Choy, V. J.; O'Connor, C. J. *Coord. Chem. Rev.* **1972**, *9*, 145. (b) Valentine, J. S. *Chem. Rev.* **1973**, *73*, 235.
(19) Vaska, L. *Acc. Chem. Res.* **1976**, *9*, 175.
(20) Igersheim, F.; Mimoun, H. *J. Chem. Soc., Chem. Commun.* **1978**, 559.
(21) (a) van Gaal, H.; Cuppers, H. G. A. M.; van der Ent, A. *J. Chem. Soc. D: Chem. Commun.* **1970**, 1694. (b) van der Ent, A.; Onderdelinden, A. L. *Inorg. Chim. Acta* **1973**, *7*, 203.
(22) (a) Louw, W. J.; Gerber, T. I. A.; de Waal, D. J. A. *J. Chem. Soc., Chem. Commun.* **1980**, 760. (b) de Waal, D. J. A.; Gerber, T. I. A.; Louw, W. J.; van Eldik, R. *Inorg. Chem.* **1982**, *21*, 2002.
(23) Vigalok, A.; Shimon, L. J. W.; Milstein, D. *Chem. Commun.* **1996**, 1673.
(24) de Bruin, B.; Peters, T. P. J.; Wilting, J. B. M.; Thewissen, S.; Smits, J. M. M.; Gal, A. W. *Eur. J. Inorg. Chem.* **2002**, 2671.
(25) Brown, J. M.; John, R. A.; Lucy, A. R. *J. Organomet. Chem.* **1985**, *279*, 245.
(26) Rohde, J.-U.; Kelley, M. R.; Lee, W.-T. *Inorg. Chem.* **2008**, *47*, 11461.
(27) Bailey, P. J.; Pace, S. *Coord. Chem. Rev.* **2001**, *214*, 91.
(28) (a) Lu, Z.; Yap, G. P. A.; Richeson, D. S. *Organometallics* **2001**, *20*, 706. (b) Duncan, A. P.; Mullins, S. M.; Arnold, J.; Bergman, R. G. *Organometallics* **2001**, *20*, 1808. (c) Mullins, S. M.; Duncan, A. P.; Bergman, R. G.; Arnold, J. *Inorg. Chem.* **2001**, *40*, 6952. (d) Bailey, P. J.; Grant, K. J.; Mitchell, L. A.; Pace, S.; Parkin, A.; Parsons, S. *J. Chem. Soc., Dalton Trans.* **2000**, 1887. (e) Bazinet, P.; Wood, D.; Yap, G. P. A.; Richeson, D. S. *Inorg. Chem.* **2003**, *42*, 6225. (f) Soria, D. B.; Grundy, J.; Coles, M. P.; Hitchcock, P. B. *J. Organomet. Chem.* **2005**, *690*, 2278. (g) Wilder, C. B.; Reitfort, L. L.; Abboud, K. A.; McElwee-White, L. *Inorg. Chem.* **2006**, *45*, 263. (h) Rische, D.; Baunemann, A.; Winter, M.; Fischer, R. A. *Inorg. Chem.* **2006**, *45*, 269.
(29) (a) Hirotsu, M.; Fontaine, P. P.; Zavalij, P. Y.; Sita, L. R. *J. Am. Chem. Soc.* **2007**, *129*, 12690. (b) Yonke, B. L.; Keane, A. J.; Zavalij, P. Y.; Sita, L. R. *Organometallics* **2012**, *31*, 345.
(30) Rohde, J.-U.; Lee, W.-T. *J. Am. Chem. Soc.* **2009**, *131*, 9162.
(31) Ogata, K.; Oka, O.; Toyota, A.; Suzuki, N.; Fukuzawa, S.-i. *Synlett* **2008**, 2663.
(32) Blackwell, J. M.; Lavoie, A. R.; Morrison, D. J.; Barrow, B. U.S. Patent 2008/0160176, July 3, 2008.
(33) (a) Fandos, R.; Otero, A.; Rodriguez, A.; Terreros, P. *Collect. Czech. Chem. Commun.* **2007**, *72*, 579. (b) Jones, C.; Mills, D. P.; Stasch, A. *Dalton Trans.* **2008**, 4799.
(34) Jones, C.; Schulten, C.; Rose, R. P.; Stasch, A.; Aldridge, S.; Woodul, W. D.; Murray, K. S.; Moubaraki, B.; Brynda, M.; La Macchia, G.; Gagliardi, L. *Angew. Chem., Int. Ed.* **2009**, *48*, 7406.
(35) Jones, C.; Schulten, C.; Fohlmeister, L.; Stasch, A.; Murray, K. S.; Moubaraki, B.; Kohl, S.; Ertem, M. Z.; Gagliardi, L.; Cramer, C. J. *Chem.—Eur. J.* **2011**, *17*, 1294.
(36) Noor, A.; Glatz, G.; Müller, R.; Kaupp, M.; Demeshko, S.; Kempe, R. *Z. Anorg. Allg. Chem.* **2009**, *635*, 1149.
(37) (a) Cotton, F. A.; Feng, X.; Timmons, D. J. *Inorg. Chem.* **1998**, *37*, 4066. (b) Irwin, M. D.; Abdou, H. E.; Mohamed, A. A.; Fackler, J. P., Jr. *Chem. Commun.* **2003**, 2882. (c) Mohamed, A. A.; Mayer, A. P.; Abdou, H. E.; Irwin, M. D.; Perez, L. M.; Fackler, J. P., Jr. *Inorg. Chem.* **2007**, *46*, 11165. (d) Coyle, J. P.; Monillas, W. H.; Yap, G. P. A.; Barry, S. T. *Inorg. Chem.* **2008**, *47*, 683.
(38) Kelley, M. R.; Rohde, J.-U. *Chem. Commun.* **2012**, *48*, 2876.
(39) Armarego, W. L. F.; Chai, C. L. L. *Purification of Laboratory Chemicals*, 6th ed.; Butterworth-Heinemann: Oxford, U.K., 2009.
(40) Herde, J. L.; Lambert, J. C.; Senoff, C. V. *Inorg. Synth.* **1974**, *15*, 18.
(41) Uson, R.; Oro, L. A.; Cabeza, J. A. *Inorg. Synth.* **1985**, *23*, 126.
(42) Wanninger-Weiss, C.; Wagenknecht, H.-A. *Eur. J. Org. Chem.* **2008**, 64.

(43) Valentini, M.; Pregosin, P. S.; Rüegger, H. *Organometallics* **2000**, *19*, 2551.
(44) Natarajan, A.; Guo, Y.; Arthanari, H.; Wagner, G.; Halperin, J. A.; Chorev, M. *J. Org. Chem.* **2005**, *70*, 6362.
(45) Yang, D.; Chen, Y.-C.; Zhu, N.-Y. *Org. Lett.* **2004**, *6*, 1577.
(46) Investigation of reaction progress by UV−Vis and ^{1}H NMR spectroscopy showed that a reaction time of 3 h is critical for full formation of **1c**. (Intermediates were not observed.) It appears that the earlier UV−Vis data stemmed from a batch of incompletely formed product. We also have revised the value for the half-life of the reaction of **1c** with O_2 (Section 3.5).
(47) Ge, S.; Meetsma, A.; Hessen, B. *Organometallics* **2008**, *27*, 3131.
(48) Hooft, R. W. W. *Collect*; Nonius BV: Delft, The Netherlands, 1998.
(49) Otwinowski, Z.; Minor, W. *Methods Enzymol.* **1997**, *276*, 307.
(50) *SHELXTL: Program Library for Structure Solution and Molecular Graphics*, version 6.12; Bruker Analytical X-Ray Systems, Inc.: Madison, WI, 2001.
(51) Sheldrick, G. M. *Acta Crystallogr., Sect. A: Found. Crystallogr.* **2008**, *A64*, 112.
(52) Walter, W.; Randau, G. *Justus Liebigs Ann. Chem.* **1969**, *722*, 52.
(53) Srinivasan, N.; Ramadas, K. *Tetrahedron Lett.* **2001**, *42*, 343.
(54) (a) Ramadas, K.; Srinivasan, N. *Tetrahedron Lett.* **1995**, *36*, 2841. (b) Ramadas, K.; Janarthanan, N.; Pritha, R. *Synlett* **1997**, 1053. (c) Berlinck, R. G. S.; Kossuga, M. H.; Nascimento, A. M. *Sci. Synth.* **2005**, *18*, 1077.
(55) Zepik, H. H.; Benner, S. A. *J. Org. Chem.* **1999**, *64*, 8080.
(56) Kresze, G.; Hatjiissaak, A. *Phosphorus Sulfur Relat. Elem.* **1986**, *29*, 41.
(57) Briefly mentioned was also the formation of the guanidines ArN=C(NR_2)NHAr, where R = Me or Et and Ar = 4-MeC_6H_4, by insertion of bis(4-methylphenyl)carbodiimide into [Ti(NMe_2)$_4$] or *N*,*N*-diethylaminoboranes, followed by methanolysis: (a) Chandra, G.; Jenkins, A. D.; Lappert, M. F.; Srivastava, R. C. *J. Chem. Soc. A* **1970**, 2550. (b) Jefferson, R.; Lappert, M. F.; Prokai, B.; Tilley, B. P. *J. Chem. Soc. A* **1966**, 1584.
(58) (a) Aeilts, S. L.; Coles, M. P.; Swenson, D. C.; Jordan, R. F.; Young, V. G., Jr. *Organometallics* **1998**, *17*, 3265. (b) Wood, D.; Yap, G. P. A.; Richeson, D. S. *Inorg. Chem.* **1999**, *38*, 5788. (c) Giesbrecht, G. R.; Shafir, A.; Arnold, J. *J. Chem. Soc., Dalton Trans.* **1999**, 3601. (d) Jin, G.; Jones, C.; Junk, P. C.; Lippert, K.-A.; Rose, R. P.; Stasch, A. *New J. Chem.* **2009**, *33*, 64. (e) Jones, C. *Coord. Chem. Rev.* **2010**, *254*, 1273.
(59) (a) Angell, C. L.; Sheppard, N.; Yamaguchi, A.; Shimanouchi, T.; Miyazawa, T.; Mizushima, S. *Trans. Faraday Soc.* **1957**, *53*, 589. (b) Mecke, R., Sr; Kutzelnigg, W. *Spectrochim. Acta* **1960**, *16*, 1225. (c) Sension, R. J.; Hudson, B.; Callis, P. R. *J. Phys. Chem.* **1990**, *94*, 4015.
(60) Albinati, A.; Bovens, M.; Rüegger, H.; Venanzi, L. M. *Inorg. Chem.* **1997**, *36*, 5991.
(61) Bernskoetter, W. H.; Lobkovsky, E.; Chirik, P. J. *Organometallics* **2005**, *24*, 6250.
(62) Ho, J. H. H.; Black, D. S. C.; Messerle, B. A.; Clegg, J. K.; Turner, P. *Organometallics* **2006**, *25*, 5800.
(63) Adams, C. J.; Anderson, K. M.; Charmant, J. P. H.; Connelly, N. G.; Field, B. A.; Hallett, A. J.; Horne, M. *Dalton Trans.* **2008**, 2680.
(64) McBee, J. L.; Escalada, J.; Tilley, T. D. *J. Am. Chem. Soc.* **2009**, *131*, 12703.
(65) Chen, F.; Sun, J.-F.; Li, T.-Y.; Chen, X.-T.; Xue, Z.-L. *Organometallics* **2011**, *30*, 2006.
(66) Gussenhoven, E. M.; Olmstead, M. M.; Fettinger, J. C.; Balch, A. L. *Inorg. Chem.* **2008**, *47*, 4570.
(67) Lahoz, F. J.; Tiripicchio, A.; Tiripicchio Camellini, M.; Oro, L. A.; Pinillos, M. T. *J. Chem. Soc., Dalton Trans.* **1985**, 1487.
(68) (a) Cotton, F. A.; Poli, R. *Inorg. Chim. Acta* **1986**, *122*, 243. (b) Ciriano, M. A.; Perez-Torrente, J. J.; Oro, L. A. *J. Organomet. Chem.* **1993**, *445*, 267. (c) Kanematsu, N.; Ebihara, M.; Kawamura, T. *Inorg. Chim. Acta* **1999**, *292*, 244. (d) Oro, L. A.; Ciriano, M. A.; Perez-Torrente, J. J.; Villarroya, B. E. *Coord. Chem. Rev.* **1999**, *193*−*195*, 941. (e) Patra, S. K.; Rahaman, S. M. W.; Majumdar, M.; Sinha, A.; Bera, J. K. *Chem. Commun.* **2008**, 2511.
(69) (a) Abel, E. W.; Skittrall, S. J. *J. Organomet. Chem.* **1980**, *193*, 389. (b) Connelly, N. G.; Garcia, G. *J. Chem. Soc., Dalton Trans.* **1987**, 2737.
(70) (a) Pregosin, P. S.; Kumar, P. G. A.; Fernandez, I. *Chem. Rev.* **2005**, *105*, 2977. (b) Macchioni, A.; Ciancaleoni, G.; Zuccaccia, C.; Zuccaccia, D. *Chem. Soc. Rev.* **2008**, *37*, 479.
(71) Valentini, M.; Pregosin, P. S.; Rüegger, H. *J. Chem. Soc., Dalton Trans.* **2000**, 4507.
(72) (a) Chianese, A. R.; Li, X.; Janzen, M. C.; Faller, J. W.; Crabtree, R. H. *Organometallics* **2003**, *22*, 1663. (b) Diebolt, O.; Fortman, G. C.; Clavier, H.; Slawin, A. M. Z.; Escudero-Adan, E. C.; Benet-Buchholz, J.; Nolan, S. P. *Organometallics* **2011**, *30*, 1668.
(73) (a) Chianese, A. R.; Kovacevic, A.; Zeglis, B. M.; Faller, J. W.; Crabtree, R. H. *Organometallics* **2004**, *23*, 2461. (b) Leuthäußer, S.; Schwarz, D.; Plenio, H. *Chem.—Eur. J.* **2007**, *13*, 7195. (c) Wolf, S.; Plenio, H. *J. Organomet. Chem.* **2009**, *694*, 1487. (d) Kelly, R. A., III; Clavier, H.; Giudice, S.; Scott, N. M.; Stevens, E. D.; Bordner, J.; Samardjiev, I.; Hoff, C. D.; Cavallo, L.; Nolan, S. P. *Organometallics* **2008**, *27*, 202. (e) Rosen, E. L.; Varnado, C. D., Jr.; Tennyson, A. G.; Khramov, D. M.; Kamplain, J. W.; Sung, D. H.; Cresswell, P. T.; Lynch, V. M.; Bielawski, C. W. *Organometallics* **2009**, *28*, 6695. (f) Dröge, T.; Glorius, F. *Angew. Chem., Int. Ed.* **2010**, *49*, 6940.
(74) (a) Crabtree, R. H.; Morris, G. E. *J. Organomet. Chem.* **1977**, *135*, 395. (b) Crabtree, R. H.; Morehouse, S. M. *Inorg. Chem.* **1982**, *21*, 4210. (c) Bucher, U. E.; Currao, A.; Nesper, R.; Rüegger, H.; Venanzi, L. M.; Younger, E. *Inorg. Chem.* **1995**, *34*, 66.
(75) Fernandez, M. J.; Rodriguez, M. J.; Oro, L. A. *Polyhedron* **1991**, *10*, 1595.
(76) Karshtedt, D.; Bell, A. T.; Tilley, T. D. *Organometallics* **2006**, *25*, 4471.
(77) Baird, B.; Pawlikowski, A. V.; Su, J.; Wiench, J. W.; Pruski, M.; Sadow, A. D. *Inorg. Chem.* **2008**, *47*, 10208.
(78) Pawlikowski, A. V.; Gray, T. S.; Schoendorff, G.; Baird, B.; Ellern, A.; Windus, T. L.; Sadow, A. D. *Inorg. Chim. Acta* **2009**, *362*, 4517.
(79) Tanke, R. S.; Crabtree, R. H. *Inorg. Chem.* **1989**, *28*, 3444.
(80) Ball, R. G.; Ghosh, C. K.; Hoyano, J. K.; McMaster, A. D.; Graham, W. A. G. *J. Chem. Soc., Chem. Commun.* **1989**, 341.
(81) (a) Sowa, J. R., Jr.; Angelici, R. J. *J. Am. Chem. Soc.* **1991**, *113*, 2537. (b) Blais, M. S.; Rausch, M. D. *J. Organomet. Chem.* **1995**, *502*, 1.
(82) Ligand acronyms: $H_2B(pz)_2$, dihydrobis(1-pyrazolyl)borate(1−); $H_2B(pz^{Me2})_2$, bis(3,5-dimethylpyrazol-1-yl)dihydroborate(1−); $BDI^{Xyl,Me}$, *N*,*N*′-bis(2,6-dimethylphenyl)pentane-2,4-diiminate(1−); $BDI^{Dipp,Me}$, *N*,*N*′-bis(2,6-diisopropylphenyl)pentane-2,4-diiminate(1−); $BDI^{Dipp,CF3}$, *N*,*N*′-bis(2,6-diisopropylphenyl)-1,1,1,5,5,5-hexafluoropentane-2,4-diiminate(1−); PyInd, 2-(2-pyridyl)indolide(1−); $PyPyr^{Ph2}$, 3,5-diphenyl-2-(2-pyridyl)pyrrolide(1−); $guan^{Ph,Me}$, *N*,*N*-dimethyl-*N*′,*N*″-diphenylguanidinate(1−); $guan^{Xyl,Me}$, *N*,*N*-dimethyl-*N*′,*N*″-bis(2,6-dimethylphenyl)guanidinate(1−); $guan^{iPr,iPr}$, *N*,*N*,*N*′,*N*″-tetraisopropylguanidinate(1−); $H_2B(I^tBu)_2$, bis(3-*tert*-butylimidazolin-1-yl-2-ylidene)dihydroborate(1−); $F_2B(I^tBu)_2$, bis(3-*tert*-butylimidazolin-1-yl-2-ylidene)difluoroborate(1−); $B(pz)_4$, tetrakis(1-pyrazolyl)borate(1−); Tp, hydrotris(1-pyrazolyl)borate(1−); Tp^{Me2}, tris(3,5-dimethylpyrazol-1-yl)hydroborate(1−); Tp^{iPr2}, tris(3,5-diisopropylpyrazol-1-yl)hydroborate(1−); To^P, tris[(4*S*)-4-isopropyl-2-oxazolinyl]phenylborate(1−); To^M, tris(4,4-dimethyl-2-oxazolinyl)phenylborate(1−).
(83) Camerano, J. A.; Sämann, C.; Wadepohl, H.; Gade, L. H. *Organometallics* **2011**, *30*, 379.
(84) de Bruin, B.; Kicken, R. J. N. A. M.; Suos, N. F. A.; Donners, M. P. J.; den Reijer, C. J.; Sandee, A. J.; de Gelder, R.; Smits, J. M. M.; Gal, A. W.; Spek, A. L. *Eur. J. Inorg. Chem.* **1999**, 1581.
(85) (a) Kutlescha, K.; Irrgang, T.; Kempe, R. *New J. Chem.* **2010**, *34*, 1954. (b) Irrgang, T.; Friedrich, D.; Kempe, R. *Angew. Chem., Int. Ed.* **2011**, *50*, 2183.
(86) Clauti, G.; Zassinovich, G.; Mestroni, G. *Inorg. Chim. Acta* **1986**, *112*, 103.

(87) (a) Field, L. D.; Messerle, B. A.; Rehr, M.; Soler, L. P.; Hambley, T. W. *Organometallics* **2003**, *22*, 2387. (b) Dabb, S. L.; Ho, J. H. H.; Hodgson, R.; Messerle, B. A.; Wagler, J. *Dalton Trans.* **2009**, 634.
(88) Goldman, A. S.; Krogh-Jespersen, K. *J. Am. Chem. Soc.* **1996**, *118*, 12159.
(89) (a) Reed, C. A.; Roper, W. R. *J. Chem. Soc., Dalton Trans.* **1973**, 1370. (b) Lebel, H.; Ladjel, C.; Belanger-Gariepy, F.; Schaper, F. *J. Organomet. Chem.* **2008**, *693*, 2645.
(90) (a) Clark, G. R.; Lu, G.-L.; Roper, W. R.; Wright, L. J. *Organometallics* **2007**, *26*, 2167. (b) Khairul, W. M.; Fox, M. A.; Zaitseva, N. N.; Gaudio, M.; Yufit, D. S.; Skelton, B. W.; White, A. H.; Howard, J. A. K.; Bruce, M. I.; Low, P. J. *Dalton Trans.* **2009**, 610. (c) Dutta, D. K.; Deb, B.; Sarmah, B. J.; Woollins, J. D.; Slawin, A. M. Z.; Fuller, A. L.; Randall, R. A. M. *Eur. J. Inorg. Chem.* **2011**, 835.
(91) Williams, D. B.; Kaminsky, W.; Mayer, J. M.; Goldberg, K. I. *Chem. Commun.* **2008**, 4195.
(92) Tang, C. Y.; Smith, W.; Vidovic, D.; Thompson, A. L.; Chaplin, A. B.; Aldridge, S. *Organometallics* **2009**, *28*, 3059.
(93) Suardi, G.; Cleary, B. P.; Duckett, S. B.; Sleigh, C.; Rau, M.; Reed, E. W.; Lohman, J. A. B.; Eisenberg, R. *J. Am. Chem. Soc.* **1997**, *119*, 7716.
(94) Penner, A.; Braun, T. *Eur. J. Inorg. Chem.* **2011**, 2579.
(95) (a) Horn, R. W.; Weissberger, E.; Collman, J. P. *Inorg. Chem.* **1970**, *9*, 2367. (b) Valentine, J.; Valentine, D., Jr.; Collman, J. P. *Inorg. Chem.* **1971**, *10*, 219.
(96) Meier, G.; Braun, T. *Angew. Chem., Int. Ed.* **2011**, *50*, 3280.
(97) Nakamoto, K. *Infrared and Raman Spectra of Inorganic and Coordination Compounds, Part B: Applications in Coordination, Organometallic, and Bioinorganic Chemistry*, 6th ed.; John Wiley & Sons: Hoboken, NJ, 2009.
(98) Hayward, P. J.; Blake, D. M.; Wilkinson, G.; Nyman, C. J. *J. Am. Chem. Soc.* **1970**, *92*, 5873.
(99) (a) Lawson, H. J.; Atwood, J. D. *J. Am. Chem. Soc.* **1988**, *110*, 3680. (b) Lawson, H. J.; Atwood, J. D. *J. Am. Chem. Soc.* **1989**, *111*, 6223.
(100) Because this reaction is slow even in the presence of an excess of CO, its scope is limited by competing self-decay. Products from self-decay of **3a** were detected by ESI mass spectrometry (cf. the Experimental Section).
(101) Verat, A. Y.; Fan, H.; Pink, M.; Chen, Y. S.; Caulton, K. G. *Chem.—Eur. J.* **2008**, *14*, 7680.
(102) Krom, M.; Coumans, R. G. E.; Smits, J. M. M.; Gal, A. W. *Angew. Chem., Int. Ed.* **2002**, *41*, 575.
(103) Any $O_2^{\bullet-}$ formed might react with the complexes present, possibly, by hydrogen atom abstraction or coordination to Ir and subsequent redox chemistry. Sawyer, D. T.; Valentine, J. S. *Acc. Chem. Res.* **1981**, *14*, 393.
(104) (a) Burrows, A. D.; Green, M.; Jeffery, J. C.; Lynam, J. M.; Mahon, M. F. *Angew. Chem., Int. Ed.* **1999**, *38*, 3043. (b) Hetterscheid, D. G. H.; de Bruin, B.; Smits, J. M. M.; Gal, A. W. *Organometallics* **2003**, *22*, 3022. (c) Hetterscheid, D. G. H.; Klop, M.; Kicken, R. J. N. A. M.; Smits, J. M. M.; Reijerse, E. J.; de Bruin, B. *Chem.—Eur. J.* **2007**, *13*, 3386.
(105) (a) Woerpel, K. A.; Bergman, R. G. *J. Am. Chem. Soc.* **1993**, *115*, 7888. (b) Ritter, J. C. M.; Bergman, R. G. *J. Am. Chem. Soc.* **1997**, *119*, 2580.
(106) Flores, J. A.; Andino, J. G.; Tsvetkov, N. P.; Pink, M.; Wolfe, R. J.; Head, A. R.; Lichtenberger, D. L.; Massa, J.; Caulton, K. G. *Inorg. Chem.* **2011**, *50*, 8121.
(107) Carlton, L.; Mokoena, L. V.; Fernandes, M. A. *Inorg. Chem.* **2008**, *47*, 8696.
(108) (a) Vaska, L.; Chen, L. S. *J. Chem. Soc. D* **1971**, 1080. (b) Brady, R.; De Camp, W. H.; Flynn, B. R.; Schneider, M. L.; Scott, J. D.; Vaska, L.; Werneke, M. F. *Inorg. Chem.* **1975**, *14*, 2669.
(109) Sciarone, T.; Hoogboom, J.; Schlebos, P. P. J.; Budzelaar, P. H. M.; de Gelder, R.; Smits, J. M. M.; Gal, A. W. *Eur. J. Inorg. Chem.* **2002**, 457.
(110) Hetterscheid, D. G. H.; Bens, M.; de Bruin, B. *Dalton Trans.* **2005**, 979.
(111) (a) Szuromi, E.; Shan, H.; Sharp, P. R. *J. Am. Chem. Soc.* **2003**, *125*, 10522. (b) Weliange, N. M.; Szuromi, E.; Sharp, P. R. *J. Am. Chem. Soc.* **2009**, *131*, 8736. (c) Wu, J.; Sharp, P. R. *Organometallics* **2009**, *28*, 6935. (d) Cinellu, M. A.; Minghetti, G.; Cocco, F.; Stoccoro, S.; Zucca, A.; Manassero, M. *Angew. Chem., Int. Ed.* **2005**, *44*, 6892.
(112) Khusnutdinova, J. R.; Newman, L. L.; Zavalij, P. Y.; Lam, Y.-F.; Vedernikov, A. N. *J. Am. Chem. Soc.* **2008**, *130*, 2174.
(113) (a) del Rio, M. P.; Ciriano, M. A.; Tejel, C. *Angew. Chem., Int. Ed.* **2008**, *47*, 2502. (b) Tejel, C.; Pilar del Rio, M.; Lopez, J. A.; Ciriano, M. A. *Chem.—Eur. J.* **2010**, *16*, 11261.